Norwegian University of Life Sciences

Master's Thesis 2017 30 ECTS
Faculty of Science and Technology

Load match study of photovoltaic production and charging demand of electric vehicles in a Zero Emission Neighbourhood – Case Campus Evenstad

Heidi Nes
Environmental Physics and Renewable Energy

Preface

This study is a master thesis which is part of the master degree in Energy and Environmental Physics at the Norwegian University of Life Sciences. The thesis studies the load match between photovoltaic production and charging demand at Campus Evenstad and is based on an initiative promoted by Sintef and The Research Centre on Zero Emission Neighbourhoods in Smart Cities (FME ZEN). Campus Evenstad is a pilot area for Sintef and FME ZEN to test solutions on how to develop and operate zero emission neighbourhoods. I find this very inspirational and I am very grateful for the opportunity to follow the work of the researchers at Sintef.

First of all, I would like to thank my supervisor at Sintef, Åse Lekang Sørensen, for enthusiastic, optimistic and dedicated guidance. I also want to thank Arne Auen Grimenes, my supervisor at NMBU, for valuable advices and feedback on my work.

Furthermore, I would like to thank Zdena Cervenka, Tarald Eng-Øvermo and Per Anders Westgaard in Statsbygg for access to inverter data and charging data for Campus Evenstad. I also want to thank Magnus Røssvold and Bjarte Aase in ABB for providing me with the charging data of ABB's charging station at Evenstad. I would like to thank Fortum Charge & Drive for answering my questions regarding the fast charging station at campus.

Finally, I would like to thank family and friends for motivation and support while writing the thesis.

Oslo, 12.12.2017

Heidi Nes

Samandrag

Campus Evenstad er ein høgskule-campus og eit pilotområde i Forskningssenter for nullutslippsområder i smarte byer (FME ZEN). FME ZEN har som mål å optimalisere energistyringa av energiproduksjon, energibehov og energilager. Denne masteroppgåva samanliknar fotovoltaisk (PV) energiproduksjon med ladeetterspurnad til elbilar som ladar på Campus Evenstad. Samanlikning av produksjon og ladebehov er nødvendig for å finne mogleg framtidig interaksjon mellom PV-produksjon og elbil-lading på campus.

Det er to ladestasjonar på campus, og i denne oppgåva blir den eine stasjonen kalla sakteladestasjon og den andre stasjonen blir kalla hurtigladestasjon. Ladeetterspurnaden på sakteladestasjonen var hovudsakleg på morgonen ifølge ladedata frå tidsrommet 01.04.2017 - 31.05.2017, medan ladeetterspurnaden på hurtigladestasjonen var fordelt utover heile dagen med størst etterspurnad på ettermiddagen ifølge ladedata frå tidsrommet 07.11.2016 - 03.09.2017. Dette tydar på at ladebehovet på campus er hovudsakleg blant tilsette og besøkande på campus.

PV-anlegget på Campus Evenstad er sørvendt og merkeeffekten er 70 kWp. PV-produksjonen på fem utvalde klare dagar i mars til og med juni blei samanlikna med tre ladeprofilar som er vald ut frå karakteristikkar ved etterspurnaden ved sakteladestasjonen. På timebasis dekker ladebehovet til dei utvalde ladeprofilane opptil 30 – 40 % av PV-produksjonen på morgonen og mindre enn 10 % av PV-produksjonen rundt kl.12.00. Den daglege PV-produksjonen er større enn den daglege energietterspurnaden til utvalde ladeprofilar for rundt 98 % av dagane i mars til og med september. Ved samanlikning av PV- produksjon og etterspurnad på hurtigladestasjonen er det tydeleg at direkte PV-dekning er avhengig av maksproduksjon rundt kl.12:00 – 13:00 på klare dagar.

Ifølge scenariovilkår er energibehovet til 7, 14 og 21 biler som ladar på campus 85 kWh, 170 kWh og 255 kWh, og dette ladebehovet er fordelt utover åtte timer mellom 08:00 og 16:00. Produksjonen på utvalde klare dagar var tilstrekkeleg til å dekke ladebehovet på timebasis unntatt mellom 08:00 – 09:00 viss 21 biler ladar dagleg. Ladebehovet i scenarioane dekte opptil 55 % av maksproduksjonen på timebasis på utvalde klare dagar. Den daglege PV-produksjonen er større enn det daglege ladebehovet til 21 biler rundt 47 % av dagane i mars til og med september ifølge PVsyst simulert produksjon for eit typisk år.

PV-produksjonsdekning av ladebehov på skya dagar avheng av skydekket i løpet av timane med ladebehov. Eit ladesystem som justerer ladeeffekten i forhold til PV-produksjonen er i nokre tilfelle nødvendig for å sikre full PV-produksjonsdekning av ladebehov på timebasis.

Ved samanlikning av PV-produksjon og ladeetterspurnad på Campus Evenstad kjem det fram at PV-produksjonen er samanfallande med funne ladebehov i arbeidstida på campus.

Abstract

Campus Evenstad is a university campus and a pilot area in The Research Centre on Zero Emission Neighbourhoods in Smart Cities (FME ZEN). FME ZEN aims to optimize the energy management of energy production, energy demand and energy storage at campus. This thesis presents a load match analysis of photovoltaic (PV) energy production and the demand of electric vehicles charging at Campus Evenstad. Studying load match is necessary to decide possibilities on future interaction between PV production and charging demand at campus.

There are two charging stations at campus and this study denotes one station as slow charging station and one station as fast charging station. The demand at the slow charging station occurred in the morning according to charging data covering 01.04.2017 – 31.05.2017, while the demand at the fast charging station was distributed throughout the day with most charging events in the afternoon according to charging data covering 7.11.2016 – 3.09.2017. This suggests that the charging demand at campus is mainly by employees and visitors at campus.

The PV plant at Campus Evenstad is oriented towards the south and the rated power is 70 kWp. The PV production on five selected clear days in March through June was compared to three charging profiles which were selected according to different characteristics of the demand at the slow charging station. The hourly demand of the selected charging profiles covered up to 30 – 40 % of the hourly morning PV production, and less than 10 % of the hourly production around PV production peak hours. The daily PV production exceeds the energy demand of the selected charging profiles for about 98 % of the days in March through September according to PVsyst simulated production of a typical year. When studying load match between PV production and the demand at the fast charging station, it is evident that instantaneous PV coverage depends on peak hour production around 12:00 – 13:00 on clear days.

Based on scenario assumptions, the energy demand of 7, 14 and 21 vehicles charging at campus is set to 85 kWh, 170 kWh and 255 kWh and the energy demand is distributed throughout eight hours between 08:00 and 16:00. The production on every selected clear day was sufficient to supply the whole hourly demand except between 08:00 – 09:00 if 21 vehicles charge daily. The scenario demands covered up to 55 % of the production during production peak hour on selected clear days. The daily PV production exceeds the scenario demand of 21 vehicles charging daily for about 47 % of the days in March through September according to PVsyst simulated production of a typical year.

The load match between PV production and charging demand on cloudy days depends on the amount of cloud cover during demand hours. A charging system which adjusts the charging power to the PV production is in some cases necessary to ensure full hourly PV coverage of charging demand.

Load match analysis shows that the PV production coincides with found charging demand during work hours at Campus Evenstad.

Nomenclature

Symbols

A	Area	m^2
A_{tot}	Total module area	m^2
E	Energy	Wh
E_m	Measured energy yield	Wh
E_s	Simulated energy yield	Wh
G_M	Irradiance on PV module	W/m^2
I	Current	A
I_{mpp}	Current at maximum power point	A
I_{SC}	Short circuit current	A
l	Length of cable	m
P	Power	W
P_{AC}	AC power	W
P_{cable}	Resistive power losses in cables	W
P_D	Local power demand	W
P_{max}	Power at the maximum power point	W
P_S	Local power supply	W
R_{cable}	Cable resistance	Ω
y	Surface Azimuth Angle	°
y_s	Solar Azimuth Angle	°
V	Voltage	V
V_{mpp}	Voltage at maximum power point	V
V_{OC}	Open circuit voltage	V
a_s	Solar altitude angle	°
β	Collector slope	°
γ_D	Self generation	-
γ_S	Self consumption	-
δ	Declination angle	°

η_{system}	System efficiency	%
θ_z	Zenith angle	°
μ	Mean	-
ρ	Specific resistivity	$\Omega \cdot \text{m}$
σ	Specific conductance	$(\Omega \cdot \text{m})^{-1}$
σ	Standard deviation	-
τ_1	Start time	s
τ_2	End time	s

Abbreviations

AC	Alternating current
AM	Air mass
BOS	Balance of system
DC	Direct current
EV	Electric vehicle
IAM	Incident angle modifier
MPPT	Maximum power point tracker
PV	Photovoltaic
SOC	State of charge
STC	Standard Test Conditions
UTC	Universal Time Coordinated
V2G	Vehicle-to-grid

Contents

1. Introduction

1.1 Background and motivation

1.1.1 Greenhouse gas emissions

The latest assessment report [1] from the Intergovernmental Panel on Climate Change (IPCC) concludes that human influence on the climate system is clear and states that recent greenhouse gas emissions have never been higher. The emissions have led to observed changes such as warmed atmosphere and oceans, diminishing snow and ice, rising sea level and more extreme weather. The report state that:

"Continued emission of greenhouse gases will cause further warming and long-lasting changes in all components of the climate system, increasing the likelihood of severe, pervasive and irreversible impacts for people and ecosystems. Limiting climate change would require substantial and sustained reductions in greenhouse gas emissions which, together with adaptation, can limit climate change risks." [1]

Large-scale adoption of renewable energy technologies is necessary to make the transition to a low carbon society. Renewable energy and electric cars are identified to be an integral part of future power systems, but an efficient incorporation of the associated technologies into existing infrastructure depends on new energy management strategies [2, 3]. Issues related to production intermittency and overloads are challenges arising when integrating photovoltaic (PV) power production and electric vehicle (EV) demand into the grid. Studies emphasize that local measures and systems for smart charging can mitigate these issues. [2, 4]

1.1.2 FME ZEN

The Research Centre on Zero Emission Neighbourhoods in Smart Cities (FME ZEN) was established in 2017 and aims to plan, develop and operate sustainable neighbourhoods with zero greenhouse gas emissions. Sintef and NTNU are research partners in FME ZEN and the centre is funded by the Research council in Norway in addition to around 30 industry and public partners. [5] This thesis is based on an initiative by Sintef and FME ZEN.

1.1.3 Campus Evenstad: pilot area and case study

Seven areas on different locations in Norway are chosen to be pilot areas for FME ZEN. These areas are test areas for technologies and solutions developed. Campus Evenstad, which is located at Evenstad in Hedmark, is among the pilot areas and serves as case-study in this thesis.

Campus Evenstad is one of the campuses belonging to Inland Norway University of Applied Sciences and has roughly 220 students and about 70 employees [6]. Statsbygg is the property manager at Campus Evenstad which consists of 22 buildings with a total floor area of about 10 000 m^2. The campus is supplied by a combination of power and heat sources. Power sources are photovoltaic cells, CHP and grid while heat sources are CHP, solar collectors, bio-boiler and electrical boiler. Accumulator tanks to store thermal energy are installed on campus

and a battery to store electrical energy is planned. Campus Evenstad also have two EV charging stations which supply slow, semi-fast and fast charging power levels. [7]

Campus Evenstad is an interesting pilot since it allows demonstration of interaction between several power and heat sources and buildings with various user profiles. A task within FME ZEN is to investigate the opportunities for interaction between PV production and EV charging in neighbourhoods. The focus of this thesis is to study the load match between PV production and EV demand at Campus Evenstad. This is further explained in the research questions below.

1.2 Research questions

This thesis will compare production profiles of the installed PV plant at Campus Evenstad with the load profiles of EVs charging at campus. By doing this, the thesis will investigate how local PV production and EV charging demand are distributed in relation to each other throughout the day. The thesis will also look upon hypothetical scenarios where the number of EVs charging at campus is increased and study how this affects load match between the production and the demand. Production and demand measurements are used in addition to simulated production in PVsyst.

In summary, the thesis will answer the following questions:

How are PV production and EV charging demand distributed in relation to each other throughout the day at Campus Evenstad?

How is the load match between PV production and EV charging demand affected when the number of EVs charging at campus is increased?

1.3 Limitations

Different limitations to this thesis are:

- This thesis only focuses upon the possible interaction between PV production and EV load, while FME ZEN aims to investigate the interaction between a wider range of energy production sources and loads. As already mentioned, Campus Evenstad has several technologies for energy production and buildings with different user profiles in addition to the EV load. It is important for FME ZEN to look upon all the different energy sources and user needs to find the most optimal energy management within the pilot area, but this is beyond the scope of this thesis.

- A stationary battery would improve the load match in a PV - EV charging system. Possibilities by including a stationary battery are not investigated in this thesis.

2. Theoretical prerequisites

This chapter is divided into three subchapters. Subchapter 2.1 describes the different parts that build a PV system and the different factors regarding irradiance and losses which impact the production. Subchapter 2.2 describes relevant aspects of charging EVs such as energy use, charging curves and charging patterns in addition to presenting smart charging strategies. Subchapter 2.3 presents an example of treating EV load as a flexible power load to utilize PV power in addition to explain load match factors.

2.1 Photovoltaic power production

Chapter 2.1 is mainly based upon *Solar Energy – Physics and engineering of photovoltaic conversion and systems* [8] and PVeducation.org [9]. Other sources are specified.

2.1.1 The PV cell and the PV array

The operation of a PV cell is based upon the principle of photovoltaic effect. The PV cell usually consists of a positive (p) and a negative (n) doped semiconductor which form a pn-junction. Photovoltaic effect occurs when the PV cell is exposed to sunlight containing photons of sufficient energy exciting electrons in the PV cell material into a higher energy state. A potential difference between the two semiconductors is generated and a direct current can be drawn from the cell by connecting an external circuit to the PV cell.

The maximum current a PV cell can deliver is the short-circuit current I_{sc} which occurs when the output connectors are shorted together. The short circuit current decreases proportionally to decreasing irradiance. The maximum voltage across a PV cell is the open voltage V_{oc} which occurs when the output connectors are not connected to a load. The open voltage decreases by increasing cell temperature. The power, P, of a PV cell is the product of the cell current I and the cell voltage V.

The *IV*-curve illustrates the relationship between the current and the voltage of an illuminated cell at a certain temperature and irradiance. The maximum power point, M_{pp}, is the point on the curve where the IV-pair, I_{mpp} and V_{mpp}, produce the maximum power, P_{max}.

Figure 2.1 illustrates the *IV*-curve and the corresponding power curve of a PV cell.

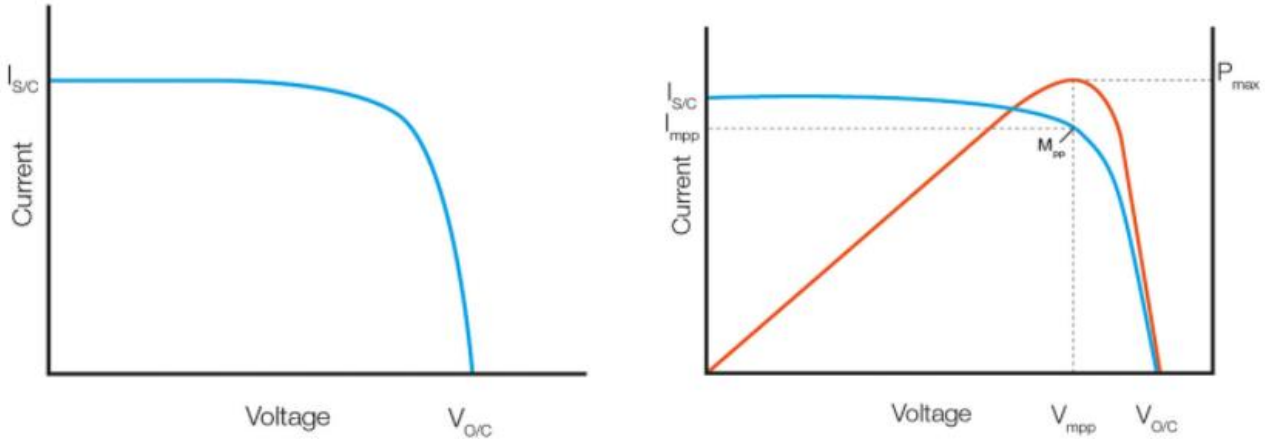

Figure 2.1 The left figure illustrates the IV-curve of a PV cell. The right figure illustrates the changing power output in response to changing current and voltage. From [10].

A silicon PV cell typically has a short circuit current of 28 – 35 $\mathrm{mA/cm^2}$ and an open circuit voltage of around 600 mV. To increase the power output, several PV cells are connected to form a module. Modules designed today often contain 60, 72 or 96 silicon PV cells connected in series. The efficiency range of commercially produced silicon cells is 16 – 24 % [11].

A PV string is a series of modules. When connecting PV strings in parallel, a PV array is formed. The output current of a PV array equals the sum of currents through each PV string and the output voltage of a PV array equals the sum of voltages of each module within a string. The array power output is the product of the array output voltage and the array output current.

Figure 2.2 illustrates a PV cell, a PV module, a PV string and a PV array.

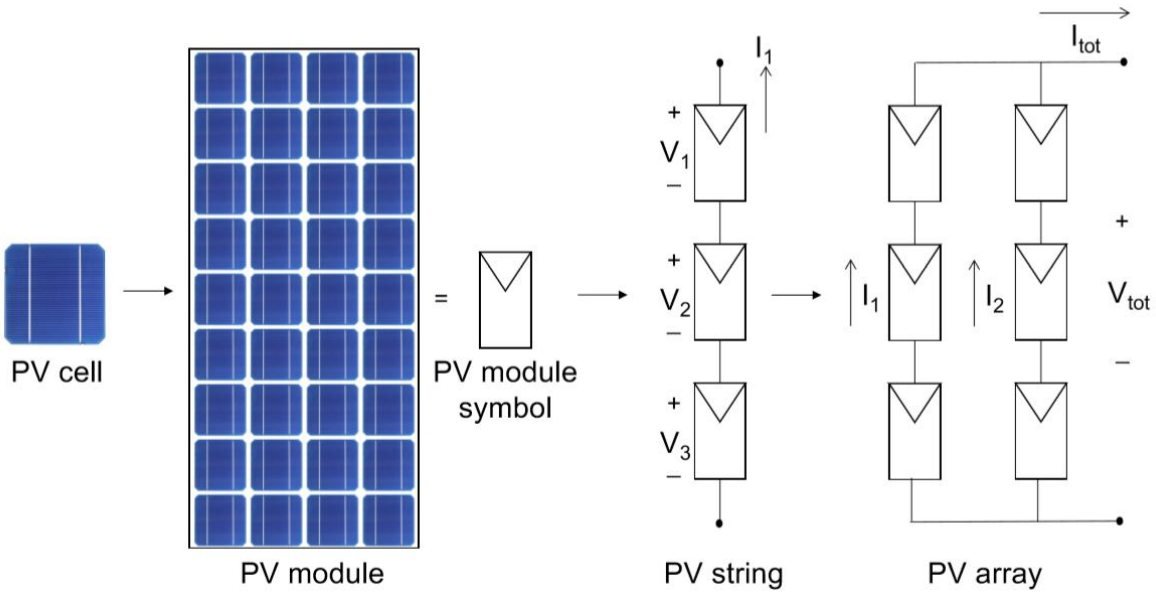

Figure 2.2. PV cell, PV module, PV string and PV array. The array output current is $I_{tot} = I_1 + I_2$. The array output voltage is $V_{tot} = V_1 + V_2 + V_3$. From [12].

2.1.2 The grid-connected PV system

Overall description

The components that build a PV system are called the *balance of system* (BOS). BOS-components of a grid-connected PV system are PV-modules, DC-AC inverters, DC-DC converters, mounting structures and cables. The DC-DC converter is usually included in the DC-AC-inverter. Figure 2.3 illustrates a grid-connected system.

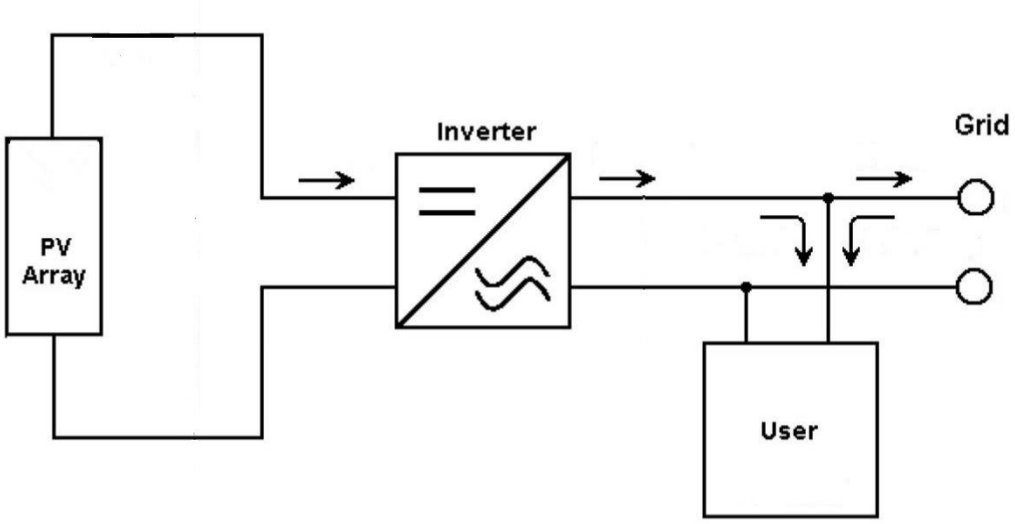

Figure 2.3. Sketch of a grid-connected system. PV power flow from the PV array to the inverter before being distributed to user loads or to the grid. In this sketch, the DC-DC converter is included in the DC-AC inverter. (=) indicates direct current and (≈) indicates alternating current. From PVsyst.

The PV array is connected to an inverter which converts the direct current, DC, produced by the PV array into alternating current, AC. The AC power are either supplied directly to the local user or fed to the grid. Usually, the power demand of the user is directly covered by PV power and the excess PV power is fed to the grid. When the PV production is insufficient to supply the total demand of the user, the deficit power is drawn from the grid.

The inverter

The inverter is usually equipped with a "Maximum Power Point Tracker" (MPPT) system. MPPT is an algorithm which aims to find the maximum power point of the array. The maximum power point of a PV array is, in the same way as for the PV cell, defined by the array current and the array voltage which produce the maximum power output. The maximum power point changes with irradiance and cell temperature and the MPPT tracks the operating point continuously for optimal operation. The included DC-DC converter adjusts the current and voltage of the PV array to match the maximum power point. The DC-DC converter also converts the PV array output voltage into a constant and compatible voltage used as input for the DC-AC inverter. The inverter is synchronized with the grid so that the phase of the AC current is in phase with the AC current of the grid. In addition, the inverter monitors the grid and is responsible for the adherence to various safety criteria [13].

The efficiency of inverters is determined by the amount of DC power converted to AC power. The efficiency of today's inverters is up to 98 % [14]. Different types of inverters decide the interconnection of PV modules and the interface with the grid. Main inverter types are centralized inverters, string inverters, multistring inverters and module inverters. Figure 2.4 illustrates the interconnection of PV modules of each inverter system.

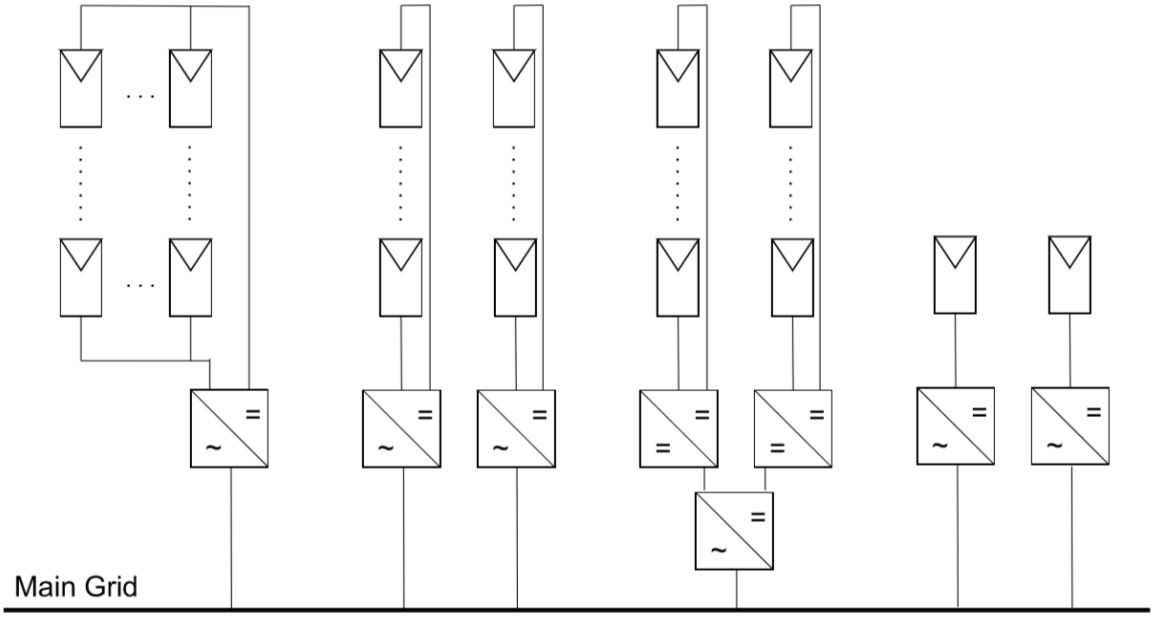

Figure 2.4. a) Centralized inverter, b) String inverter, c) Multistring inverter, d) Module inverter. (=) indicates direct current and (≈) indicates alternating current. From [12].

The centralized inverter is connected to a PV array. This configuration achieves high voltage output and the centralized inverter is used in large-scale PV systems. The specific cost of the inverter is low and the system is easier to maintain compared to other inverter systems since it consists of fewer components, but future expansion of the system is more challenging than for other inverter systems. Power losses occur due to a centralised MPPT and power losses may occur due to current mismatch between modules in strings. Current mismatch due to shading is discussed in chapter 2.1.5.

The string inverter is connected to a PV string which is operated by its own MPPT. As in the centralized inverter system, the string inverter system achieves high voltage output, but can also have power losses due to current mismatch between the modules in the string. The string inverter is often used in small systems mounted on private houses or office buildings.

The multistring inverter is connected to multiple DC-DC converters. Each DC-DC converter is connected to a PV string and each string is operated by its own MPPT. The multistring inverter system combines the advantage of low costs as for the centralized inverter system and the advantage of high energy yield as for the string inverter system. Expanding the system is also easily achieved. [15]

The module inverter is mounted directly on the module and each module operates at the maximum power point. The mismatch losses between the modules are therefore removed. Increasing or decreasing the size of the system is easily achieved, but the system is more expensive compared to other inverter systems.

Cables

Cables transfer the array power to the inverters, the loads and the grid. The resistance of the cables causes resistive losses which are described by the following formula

$$P_{\text{cable}} = I^2 R_{\text{cable}} \qquad 2.1$$

where P_{cable} is the resistive power losses, I is the current and R_{cable} is the cable resistance. The cable resistance is given by

$$R_{\text{cable}} = \rho \frac{l}{A} = \frac{1}{\sigma} \frac{l}{A} \qquad 2.2$$

where p is the specific resistivity, A is the cross section of the cable, σ is the specific conductance and l is the length of the cable.

Minimizing the resistive losses is important when designing a PV system.

2.1.3 PV module irradiance

The irradiation received outside Earth's atmosphere is 1361 W/m^2. This is called the solar constant and is defined as the average irradiation received perpendicular to Earth's atmosphere at the mean distance between the sun and Earth's atmosphere. Irradiance received on Earth's surface varies significantly with latitude, season of the year, time of the day and local variation in the atmosphere. Seasonal and diurnal irradiance fluctuations are caused by Earth's movement relative to the sun. Earth's movement and tilt relative to the sun are illustrated in figure 2.5.

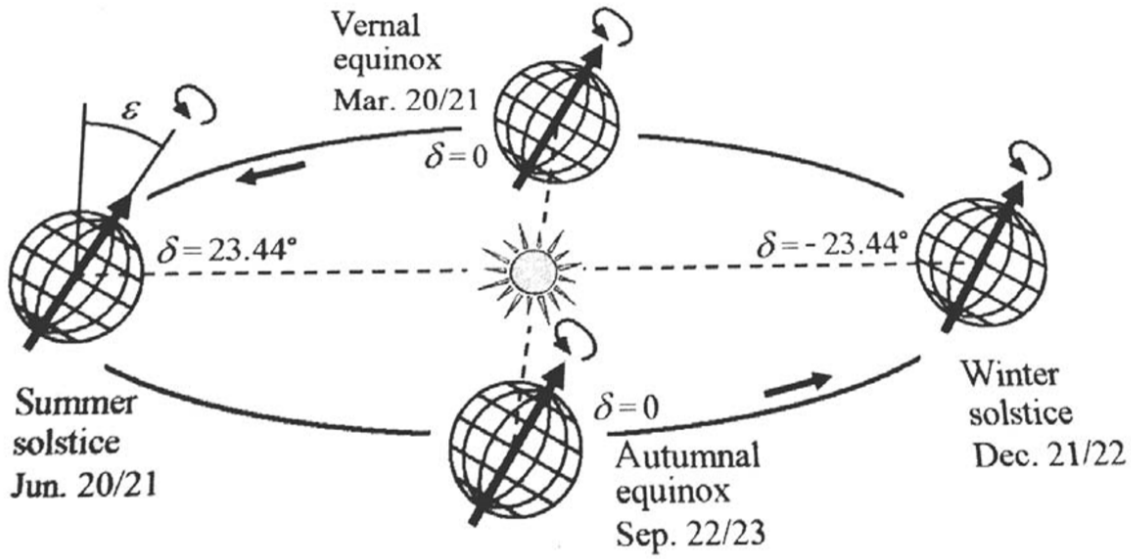

Figure 2.5. Illustration of Earth's movement around the sun throughout the year. The declination angle, δ, is the angle between the equator and a line drawn from the centre of Earth to the centre of the sun. δ vary seasonably between plus and minus 23.45 °. Summer solstice marks the day where the sun reaches the highest point above the horizon at noon in the Northern Hemisphere. Winter solstice marks the day where the sun is at its lowest point above the horizon at noon in the Northern Hemisphere. From [16].

Air mass, AM, is the ratio of the sunlight's path length through the atmosphere and the shortest path length possible. The shortest path length possible occurs when the sun is directly above the horizon. In this case, the air mass equals 1 and is denoted AM1. The amount of transmitted sunlight depends on the path length taken through the atmosphere as a portion of the sunlight become attenuated by atmosphere molecules or clouds by absorption, scattering or reflection when passing through the atmosphere. Direct irradiance describes the part of the sunlight which pass through the atmosphere in a straight line while diffuse irradiance describes the part of the sunlight which are scattered by molecules in the atmosphere.

Irradiance on a PV module depends on different angles. Figure 2.6 and table 2.1 illustrates and explains relevant angles.

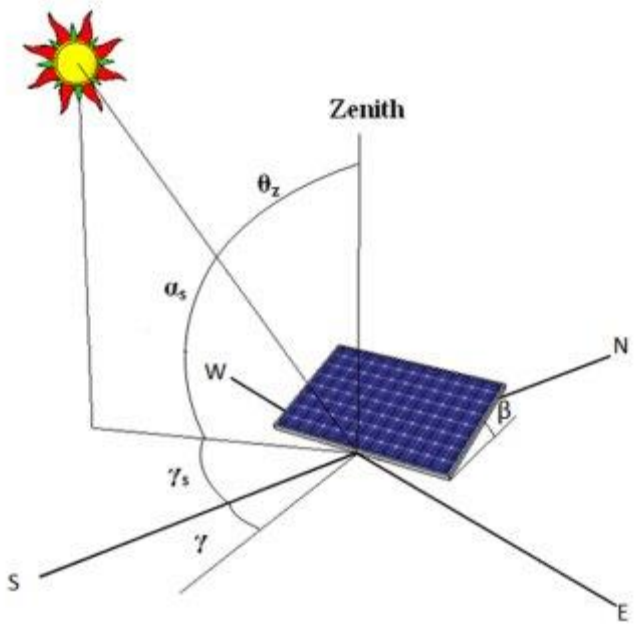

Figure 2.6. Relevant angles regarding PV module irradiance. © William Sturles, University of Colorado at Boulder.

Table 2.1. Relevant angles regarding PV module irradiance explained.

θ_z, Zenith angle	The angle between the vertical to the horizon and the line pointing to the sun.
a_s, Solar altitude angle	The angle between the horizontal and the line that points to the sun.
y_s, Solar azimuth angle	The angle between the line that points to the south and to the sun. Angles to the west are positive and the angles to the east are negative.
y, Surface azimuth angle	The angle between the line pointing to the south and the line pointing straight out of the PV module. Angles towards the west are positive and angles towards the east are negative.
β, Collector slope	The angle between the plane of the PV module and the horizontal.

As the sunlight hits Earth with an increasing zenith angle, the sunlight become distributed over a larger area. The irradiation received by the surface is consequently reduced moving from noon to evening, from summer to winter and from Equator to the poles. Figure 2.7 illustrates the impact of an increasing zenith angle on irradiation received by the surface.

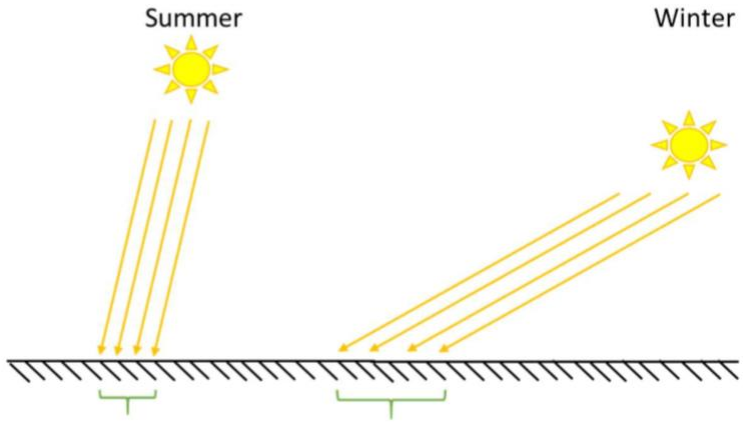

Figure 2.7. Changing irradiance received by the surface due to Earth's motion relative to the Sun. From [17].

2.1.4 PV production profiles

The instantaneous AC power output of a PV system can be described by following equation:

$$P_{\mathrm{AC}}(t) = A_{\mathrm{tot}} G_{\mathrm{M}}(t) \eta_{\mathrm{system}}(t) \qquad 2.3$$

where $P_{AC}(t)$ is the instantaneous AC power output of the system, A_{tot} is the total module area, $G_M(t)$ is the irradiance incident on the PV module and $\eta_{system}(t)$ is the system efficiency. $G_M(t)$ is the sum of direct irradiance, diffuse irradiance and irradiance reflected from the ground.

The incident irradiance on a module surface is maximum when the surface of the module and the sunlight are perpendicular to each other. However, the angle between the sun and the module's surface is continually changing. PV modules located in the Northern Hemisphere receive maximum power over the course of a year if oriented directly to the South (y = 0 °). When the modules are oriented towards the South, the power peak production occurs at noon. If the modules are oriented towards East or West, the power peak production occurs in the morning and afternoon respectively.

2.1.5 PV system performance

System performance terms
Power rating and specific yield are PV system performance terms. The power rating of a PV system, given in Watt-peak [Wp], is defined as the maximum power the PV array can produce under Standard Test Conditions (STC). The conditions that define STC are irradiance equal to 1000 $\mathrm{W/m^2}$, air mass equal to AM1.5 (θ_z= 48.2°) and cell temperature equal to 25 ℃. The specific yield, given in Wh/Wp, is the ratio of the annual yield and the rated power of the PV system. This term can be used to compare PV installations with different orientations and on different locations.

Losses
Main power losses which decide the PV system efficiency, η_{system}, are:

- Pre-photovoltaic losses due to shading of modules, soiling of modules or snow-covered modules and module surface reflection of incoming sunlight.
- Module losses due to the conversion efficiency of the cells. The efficiency of modules also decreases over time due to weather and possible damages.
- System losses due to cable resistance, inconsistent MPPT tracking, inverter efficiency and mis-sized inverter.

The effect of wind
An increasing PV cell temperature leads to cell conversion efficiency decrease as the open voltage of the cell decreases. The cooling effect of wind is therefore a positive effect on a PV system.

Reducing shading effects
The short circuit current of a cell is reduced by shading. To reduce the effect of shading, a module may be equipped with bypass diodes. A bypass diode is connected in parallel with a series connection of PV cells. The bypass diode has opposite polarity relative to the PV cells which ensures that the bypass diode does not conduct current under normal operating conditions. When there is mismatch in short-circuit current of series connected cells due to shading, the bypass diode reverses its polarity and begin conducting current. The current passes through the diode instead of the shaded PV cell. Consequently, the current of unshaded cells is prevented from going through the shaded cell.

If unshaded cells force a higher current through the shaded cell than the shaded cell can conduct, the voltage across the shaded cell may become negative. In this case, the shaded cell starts consuming power which lead to overheating of the cell.

2.2 EV charging

2.2.1 Battery terms and charging facilities

Battery terms
Two terms which describe the condition and the capacity of the EV battery are used in this thesis and these are:

Energy capacity [Wh] - Energy available when the battery is discharged from maximum capacity at a certain discharge current until the minimum allowed voltage is reached which indicates an "empty" battery. [18]

State of Charge (SOC) [%] – The present battery capacity expressed as the percentage of maximum capacity. [18]

Charging facilities
Power levels used to charge EVs are divided into slow charging power levels, semi-fast charging power levels and fast charging power levels. Slow charging power levels are power levels up to 20 kW, semi-fast charging power levels are power levels between 20 – 40 kW and fast charging power levels are power levels over 40 kW [19]. Different manufacturers have developed different types of charging connectors. For slow/semi-fast charging, the Type 2 connector are increasingly used and recommended. For fast charging, the Chademo connector, the Combo 2 Charging System (CCS2) connecter and the Tesla Supercharger connector are mainly used. [5]

The Type 2 connector has an efficiency of 95 %. The percentage of power drawn from the grid which is taken up by the EV battery is around 89 %. [20, 21]

2.2.2 Charging curve
Figure 2.8 shows a typical charging curve found by the project "Low Carbon London" [22]. The charging curve is based upon charging data of one vehicle charging at 3.7 kW where the EV battery is charged to full capacity. As the battery approaches full capacity, a gradual decrease of charging power is observed. The gradual decrease of charging power is likely caused by control actions of the battery management system as SOC approaches 100%. Charging power only decreases if the battery is charged to its full capacity. [22]

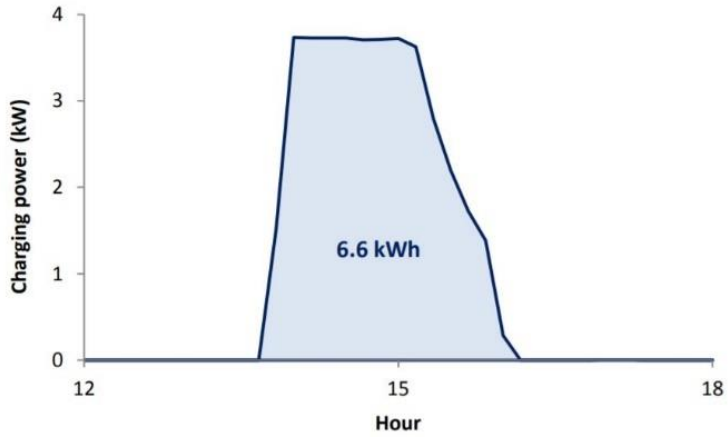

Figure 2.8. Charging curve of one vehicle found by the project "Low Carbon London" [22]. The vehicle charged at 3.7 kW for 2.5 hours and 6.6 kWh was consumed from the grid.

Fortum points out that the fast charging curve depends on many parameters such as type of car, SOC at charging start and end, battery temperature, etc. [23] Seljeseth & Taxt [24] have measured the charging demand at a fast charging station in Trondheim on a typical day in 2013. The charging station supplied up to 50 kW and figure 2.9 shows the fast charging curves and the fast charging energy consumption found by Seljeseth & Taxt [24].

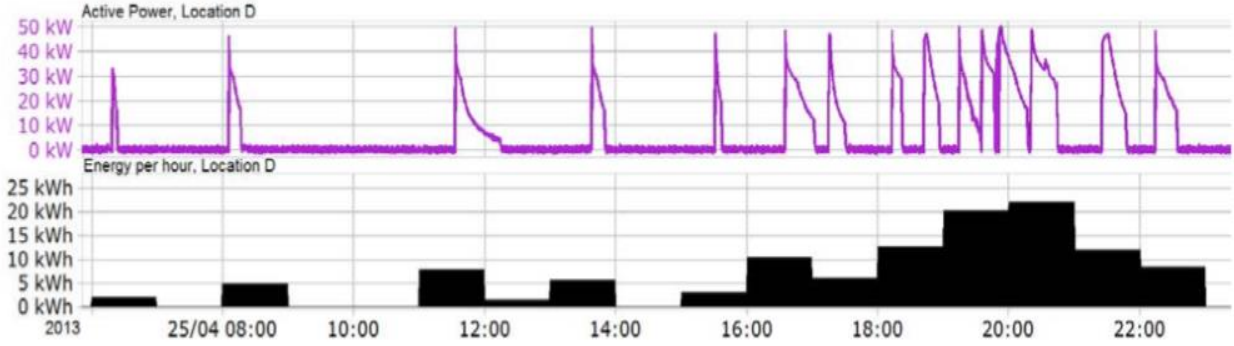

Figure 2.9. Fast charging curves and fast charging energy consumption found by Seljeseth & Taxt. [24]. The upper figure shows the measured charging curves and the lower figure shows the energy consumption of each charging curve.

2.2.3 EVs in Norway

Energy use and vehicle's energy capacity

A study of the energy use of popular EV types in Norway have found that the energy use per kilometre can be as low as 0.1 – 0.15 kWh per kilometre during summer months. The energy use per kilometre during winter months can be twice as large. [25]

The battery energy capacity of the ten most popular EVs in Norway range between 14 kWh to 100 kWh. The Nissan Leaf model which was launched in 2010 has a net battery energy capacity of 21.6 kWh which constitute a range of 100-160 km. This car type is the most sold EV in Norway today. [5, 26]

The energy capacity of EV batteries, and consequently the range of EVs, are continually increasing. Over the next three years, different manufacturers will launch vehicles with a range of above 500 km. [27]

Average charging profiles

The EV fleet in Norway is increasing. The Norwegian Water Resources and Energy Directorate (NVE) has analysed charging patterns in Norway today and made average charging profiles from charging data and surveys [25]. Using these profiles, the energy use throughout the day of 1.5 million EVs are studied. Figure 2.10 shows the energy use of 1.5 million EVs in Norway as predicted by NVE.

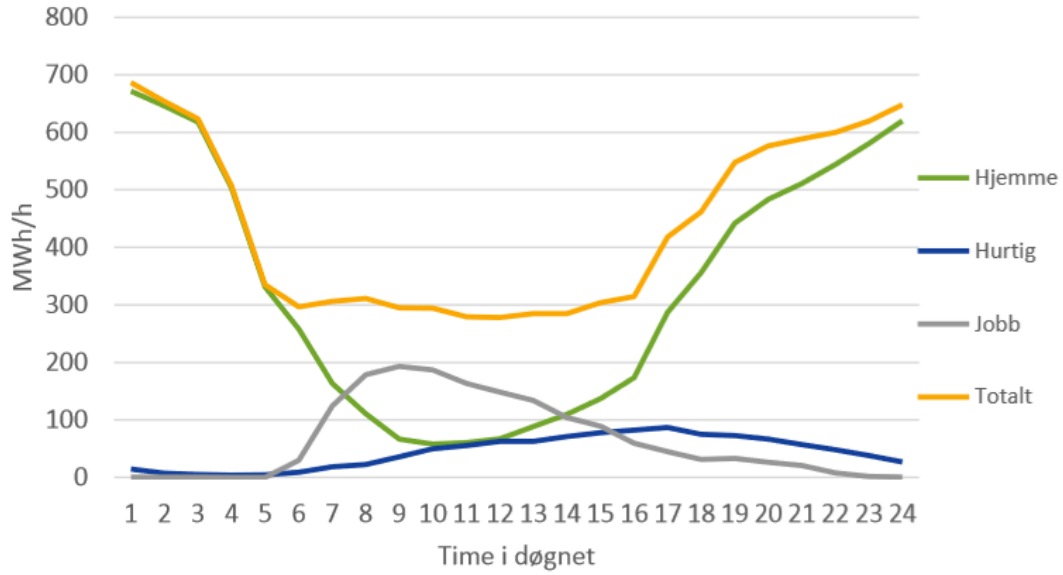

Figure 2.10. The energy use of 1.5 million EVs in Norway in 2030 throughout the day as predicted by NVE. "Hjemme"-profile represents home charging, "Hurtig"-profile represents fast charging, "Jobb"-profile represents work charging and "Totalt"-profile represents the total charging demand. The x-axis "Time i døgnet" represents the hours throughout the day. From [25].

The shape of the charging profiles depends on the charging location and can be summarized as follows:

- Home charging is mainly done during the night with a peak energy demand around 01.00.
- Fast charging is distributed throughout the day from morning until around midnight.
- Work charging begins around 06.00 and increase continually until roughly 09.00 when it starts to decrease until the end of the work day at around 17.00.

2.2.4 Smart charging

Smart EV charging systems described in literature or smart EV charging systems available at the market today vary according to various goals and specifications. Figure 2.11 shows some examples of common control strategies and goals for smart EV charging systems.

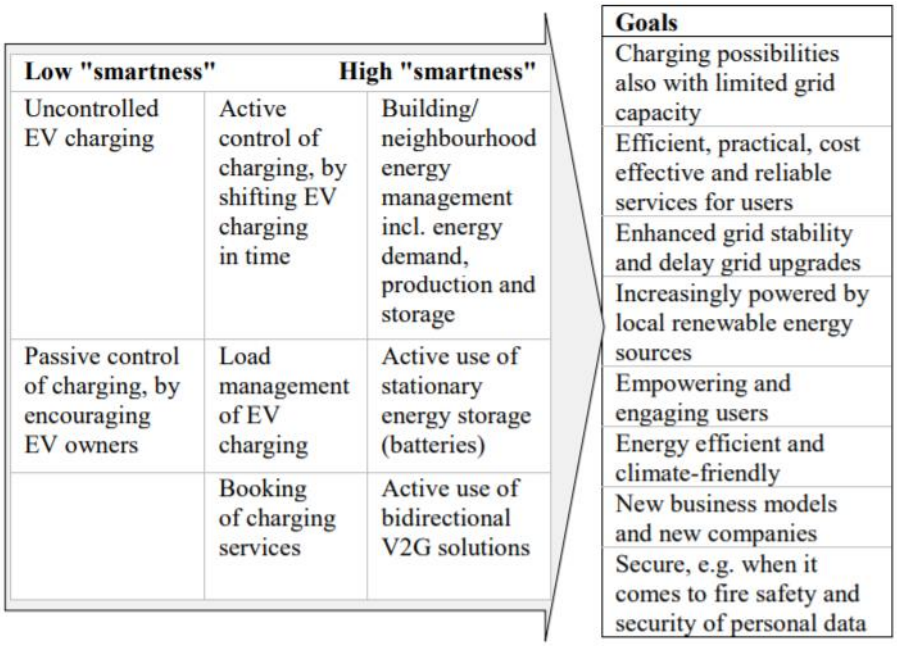

Low "smartness"		High "smartness"
Uncontrolled EV charging	Active control of charging, by shifting EV charging in time	Building/ neighbourhood energy management incl. energy demand, production and storage
Passive control of charging, by encouraging EV owners	Load management of EV charging	Active use of stationary energy storage (batteries)
	Booking of charging services	Active use of bidirectional V2G solutions

Goals
Charging possibilities also with limited grid capacity
Efficient, practical, cost effective and reliable services for users
Enhanced grid stability and delay grid upgrades
Increasingly powered by local renewable energy sources
Empowering and engaging users
Energy efficient and climate-friendly
New business models and new companies
Secure, e.g. when it comes to fire safety and security of personal data

Figure 2.11. Examples of common control strategies and goals for smart EV charging systems. From [5].

The different possibilities in figure 2.11 are sorted from low to high “smartness”. Different control strategies entails shifting EV load in time, management of demand, production and storage in a neighbourhood and use of vehicle-to-grid (V2G) solutions. The goals of smart charging include utilization of local renewable power, enhanced grid stability, activated users and cost-effective EV charging management.

2.3 EV charging from locally produced PV power

2.3.1 Controlled charging to utilize PV power

Residential load is characterized by power peak demand in the morning and in the afternoon/evening. Non-residential buildings usually have power peak demand during office hours.[26] OECD/IEA [4] illustrates in figure 2.12 a scenario where standard usage patterns of residential load are combined with EV charging load during a typical day in the European Union in 2030. By controlling the EV charging to coincide with PV production, the net peak power demand decrease by roughly one-third.

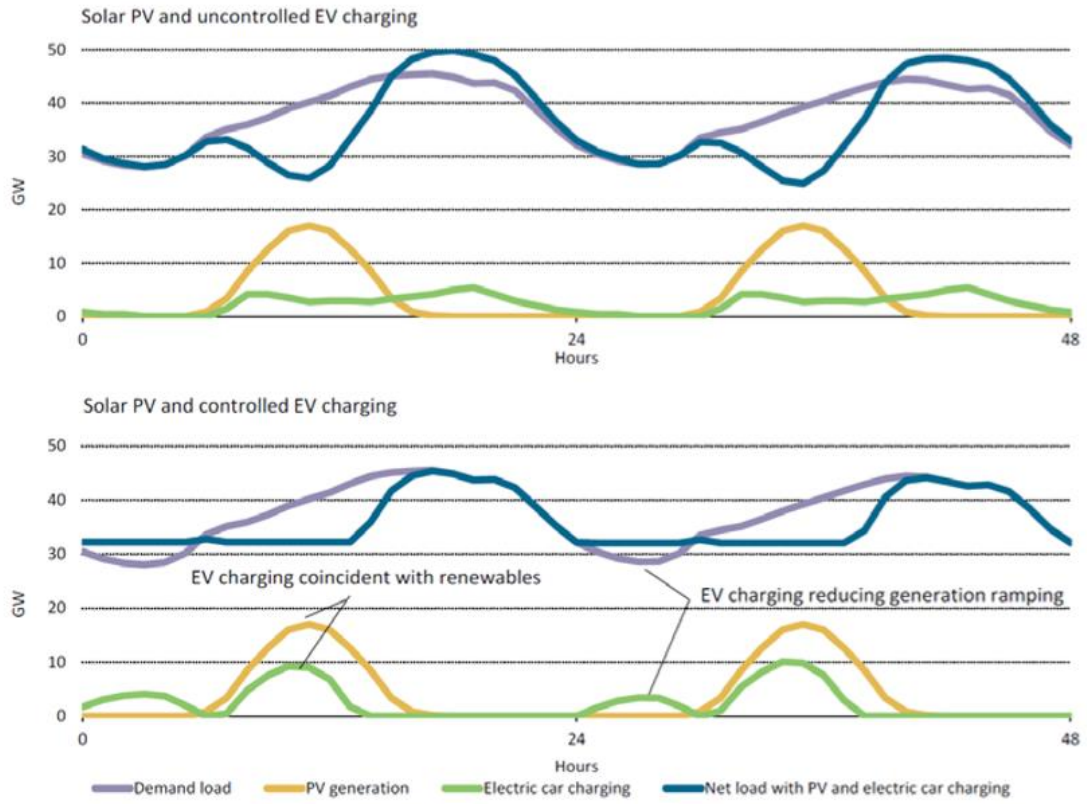

Figure 2.12. Figures based on scenario by OECD/IEA. Both figures show PV production and standard usage patterns of residential load in a typical day in the European Union in 2030. The upper figure shows uncontrolled EV charging while the lower figure shows EV charging which by control coincides with PV production. The "Net load with PV and electric car charging" curve illustrates the PV production subtracted from the sum of residential load and EV load. From [4].

EVs represent a flexible load in contrast to the many stationary loads in a neighbourhood. Private EVs are on average parked around 93–96% of their lifetime [26] and this makes EVs suited for load shifting and power adjustments over time. Adjusting the demand to the generation is called demand-side management. OECD/IEA identify EVs as well fitting to promote synergies with different renewables through demand-side management. [4]

2.3.2 Load match factors

Self-generation, γ_D, and self-consumption, γ_S, are load match factors which aim to portray the extent of utilization of locally produced energy for local energy demand. Self-generation is the fraction of demand that is covered by PV production, while self-consumption is the fraction of PV production that is covered by the demand. Self generation and self consumption are calculated using following formulas:

$$\gamma_D = \frac{\int_{\tau_1}^{\tau_2} \min[P_{\mathrm{D}}, P_{\mathrm{S}}] dt}{\int_{\tau_1}^{\tau_2} P_{\mathrm{D}}\, dt} \qquad 2.4$$

$$\gamma_S = \frac{\int_{\tau_1}^{\tau_2} \min[P_{\mathrm{D}}, P_{\mathrm{S}}] dt}{\int_{\tau_1}^{\tau_2} P_{\mathrm{S}}\, dt} \qquad 2.5$$

where P_{D} is the local power demand, P_{S} is the local power supply and the term $min[P_{\mathrm{D}}, P_{\mathrm{S}}]$ represents the part of the local power demand which is covered by the local power supply or the part of the local power supply which is covered by the local power demand. The load match factors are based on a time resolution which is described by the start time τ_1 and the end time τ_2. Self generation and self consumption can for example be calculated on a hourly, daily, monthly and annual basis. [28]

3. Methodology

This chapter starts with describing the PV system and the charging stations at Campus Evenstad. Further on, the production simulations in PVsyst are described before the selection of production and demand measurements are presented. Different scenarios which entails an increased EV demand at campus are described before the final subchapter describes how the load match between PV production and EV demand is found.

3.1 System description

3.1.1 The photovoltaic system

The photovoltaic system at Campus Evenstad was installed in November 2013 by FUSen. The system consists of 276 PV modules and 12 inverters and the rated power is 70 kWp. The annual yield expectancy is 60 MWh/year and the energy produced is directly used by the University for most of the time. [29, 30]

Each PV module is a multi-crystalline silicon module of the model 255 PE from REC Solar AS. Each module has three bypass-diodes and each bypass-diode are connected to a string of 20 PV cells which give a total of 60 PV cells per module. The maximum power output of each module at STC is 255 W and the module efficiency at STC is 15.1 %. The total area of the PV array is 455 m^2 [29, 31].

The modules are mounted on K2 Speedrail stands on the south-facing roof of the barn which has an estimated surface azimuth angle of $-10\,°$ [12]. The tilt of the roof and the collector slope of the PV array is $35\,°$ [29]. Figure 3.1 is a picture of the PV array on the roof of the barn.

Figure 3.1. The PV array on the roof of the barn at Campus Evenstad. From [32].

Cables transferring the array power are connected to DC-switches and a surge protection device before being connected to the inverters [33]. The inverters are string inverters of the model Sunny Boy 5000TL-21 from SMA Solar Technology AG (SMA). The maximum efficiency of each inverter is 97 % and the rated power is 4.6 kW. [33, 34]

Each inverter has two MPPT-inputs which allows the inverter to connect to two strings with different number of modules. Each inverter is connected to a string of eleven modules and a string of twelve modules. In total, the PV system consists of 24 strings. Each string is assigned two numbers. The first number defines which of the twelve inverters the string is connected to and the second number defines the number of modules the string consists of where "1" refers to strings with eleven modules and "2" refers to strings with twelve modules. [35] Table 3.1 shows the arrangement of the PV strings.

Table 3.1. The PV string arrangement. Each string is assigned two numbers. The first number defines which of the twelve inverters the string is connected to and the second number defines the number of modules the string consists of where "1" refers to strings with eleven modules and "2" refers to strings with twelve modules.

1.1	1.2	2.1	2.2	3.1	3.2
4.1	4.2	5.1	5.2	6.1	6.2
7.1	7.2	8.1	8.2	9.1	9.2
10.1	10.2	11.1	11.2	12.1	12.2

The inverters are connected in series to the monitoring device Sunny WebBox which continuously measure the AC power output of the inverter. In addition, Sunny WebBox collects measurements from Sunny SensorBox which is installed on the roof of the barn. Sunny SensorBox contains sensors that measure sun radiation, module temperature, wind speed and ambient temperature. These measurements along with the measurements of the inverter power output are transmitted by Sunny WebBox to the internet portal Sunny Portal where the measurements are displayed. [12]

Trees located on the west side of the PV array, a house located on the east side of the PV array and mountains in the horizon may cast shadow on the PV array at different times throughout the day.

3.1.2 The charging stations

In this thesis, the two charging stations at Campus Evenstad are addressed as "the slow charging station" and "the fast charging station". Note that both stations offer power levels which normally are addressed as semi-fast charging power levels. The demand at the slow charging station is denoted as slow charging demand and the demand at the fast charging station is denoted as fast charging demand throughout the thesis.

Slow charging station

The slow charging station at campus is delivered by Salto Ladestasjoner and has altogether four Type 2 connectors. One of these connectors supplies a power level of either 6.9 kW or 20 kW. The three remaining connectors supply a power level of either 3.5 kW or 10 kW. The charging station supplies 1 phase AC power or 3 phase AC power depending on the selected charging power. [36] The slow charging station is owned by the University [37].

Figure 3.2 is a sketch of four vehicles connected to the four connectors at the slow charging station at Campus Evenstad. Figure 3.3 is a picture of the slow charging station at Campus Evenstad.

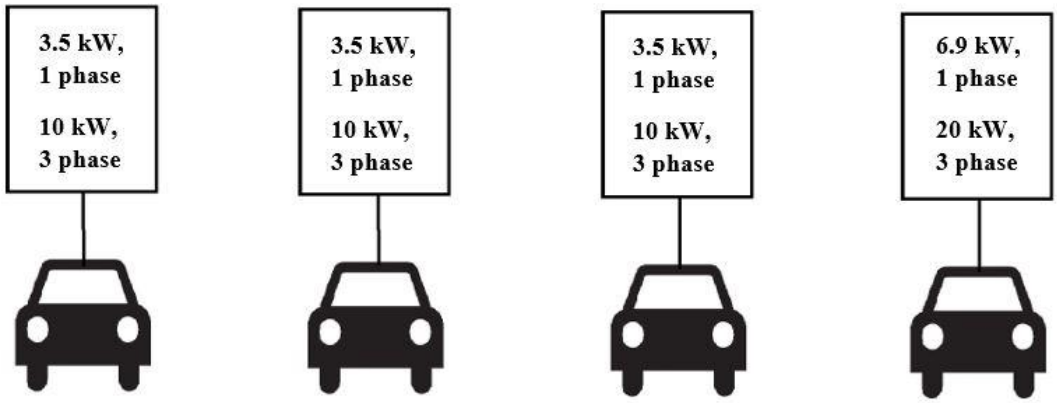

Figure 3.2. Sketch of the four connectors at the charging station at Campus Evenstad. The sketch specifies the number of phases and the charging power offered by each connector.

Figure 3.3. Picture taken of the slow charging station at Campus Evenstad.

Fast charging station

The fast charging station at Campus Evenstad consists of one station delivered by ABB and one station delivered by Efacec Electric Mobility. Both stations have one Chademo connector, one CCS/Combo connector and one Type 2 connector. The Chademo connector and the CCS/Combo connector supply a maximum DC power of 50 kW and the Type 2 connector supply a maximum AC power of 22 kW. It is not possible to use both the Chademo connector and the CCS/Combo connector simultaneously at the same station. The maximum power supply at each station is therefore 72 kW.

The fast charging station at Campus Evenstad is operated by Fortum. [38] Figure 3.4 is a sketch of the fast charging station and figure 3.5 is a picture of the station.

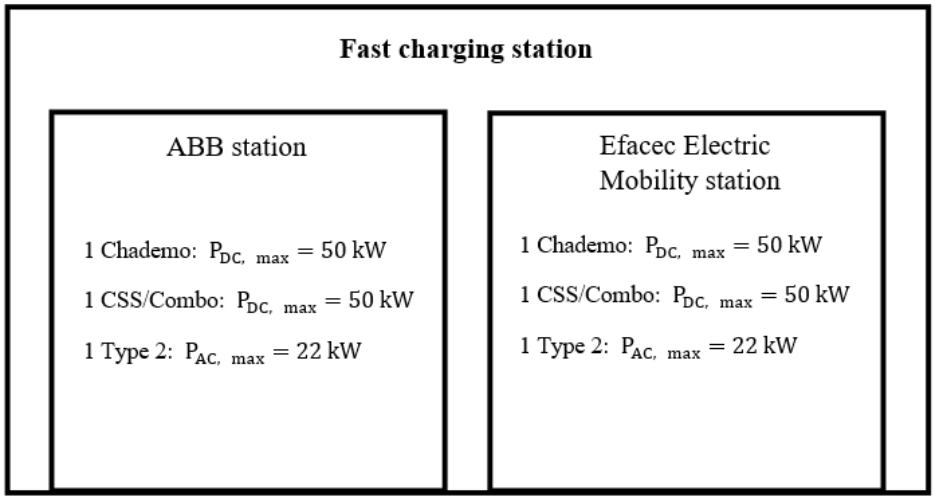

Figure 3.4. Sketch of the fast charging charging station at Campus Evenstad.

Figure 3.5. Picture taken of the fast charging station at Campus Evenstad.

3.2 PVsyst simulation

PVsyst is a software package to size, simulate and analyse complete PV systems. The PV production at Evenstad in a typical year and the PV production at Evenstad on clear days are simulated in PVsyst (version 6.49). The PVsyst simulations are used to:

- Support selection of clear example days.
- Create solar path chart for Campus Evenstad.
- Create clear day production profiles throughout the year.
- Find the percentage of days in a typical year where the PV system produce above a certain energy yield level.

The parameters used in the simulations and the uncertainties regarding the simulations are explained in chapters 3.2.1-3.2.3. The full report of the typical year simulation is given in the appendix. The parameters used in the clear day simulation are identical to the parameters used in the typical year simulation, but the two simulations are based on different meteorological data.

3.2.1 Meteorological data

Interpolated monthly meteorological values for Evenstad was generated in PVsyst using the database Meteonorm. The monthly meteorological values include irradiance values, temperature values and wind speed values [39]. Figure 3.6 shows the weather stations included in the Meteonorm database. The green markers represent weather stations which include irradiance measurements and the blue markers represent weather stations which lack irradiance measurements. Evenstad is represented by the brown marker. The interpolation of monthly meteorological values is based on the measurements between 1991 – 2010 of the closest weather stations in addition to satellite information [39].

Two meteorological data files were created; one data file containing interpolated monthly meteorological data representing a typical year at Evenstad and one data file containing interpolated monthly meteorological data for a year only consisting of clear days at Evenstad. For simulations, synthetic hourly values are used which are generated from the interpolated monthly values. Synthetic hourly data are hourly data values generated by PVsyst according to a model in a stochastic process [39].

Figure 3.6. The location of the weather station measurements which are included in Meteonorm. Green markers = weather stations with irradiance measurements. Blue markers = Weather stations without irradiance measurements. Brown marker = Evenstad. The irradiance measurements in Norway which are included in Meteonorm are measurements made in Ås, Bergen, Bodø and Tromsø. From Meteonorm.

3.2.2 Selected PVsyst parameters

The selected parameters regarding orientation, modules, inverters, IAM-values, horizon and near shading are given below.

Orientation and System

Chosen parameters for orientation and system are:

Field type	Fixed Tilted Plane
Plane tilt/azimuth	35° / -10°
PV modules:	REC 255PE/PE-BLK, Si-poly, 255 Wp 26 V
Inverters:	Sunny Boy 5000 TL-21, 4.6 kWac
Sub-array 1:	12 strings of 11 modules in series, 12 MPPT inputs
Sub-array 2:	12 strings of 12 modules in series, 12 MPPT inputs

IAM values

Incident Angle Modifier (IAM) is defined as the ratio of the module efficiency at a given angle of incidence and the module efficiency at normal incidence. The IAM values consequently identify the impact on module's performance as the angle of the sun changes relative to the module surface. [40]

The modules used at Evenstad is part of the REC Peak Energy Series. The IAM values of these modules have been tested by Solar Energy Research Institute Singapore (SERIS) [40]. Table 3.2 shows the IAM values implemented in PVsyst and the IAM values found by SERIS. The IAM values found by SERIS are used in simulations and these values contribute to a higher performance of the PV plant than the IAM values which were implemented in PVsyst originally.

Table 3.2. The IAM values which were implemented in PVsyst originally and the IAM values found by SERIS which were used in simulations.

Angle	**10°**	**30°**	**50°**	**60°**	**70°**	**75°**	**80°**
PVsyst implemented IAM values, %	100.0	99.9	98.5	95.3	87.0	79.0	67.7
IAM values found by SERIS, %	100.0	100.1	99.4	97.4	91.1	84.1	72.2

Near shading and horizon

Åsheim [12] has simulated the PV system at Campus Evenstad. This thesis uses the same horizontal line, shading objects and shading object dimensions as Åsheim. The position of the near shading objects relative to each other are estimated by measuring distances and angles in Google Maps. Figure 3.7 shows the shading scene defined in PVsyst.

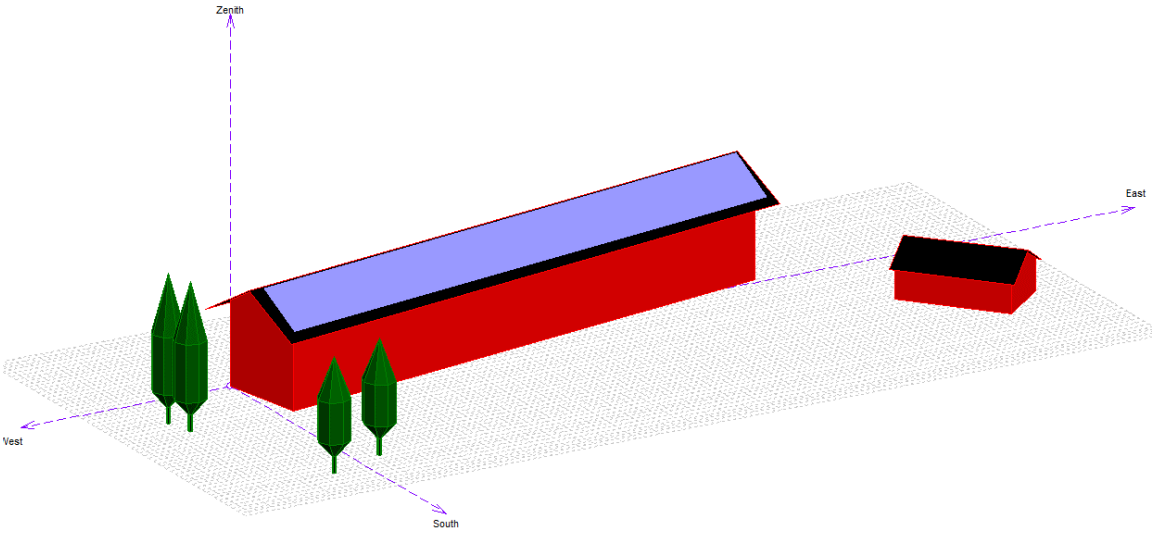

Figure 3.7. The near shading scene defined in PVsyst where the blue rectangle represents the PV array. From PVsyst.

PVsyst allows users to simulate the impact of near shading according to “linear shading” or “electrical losses”. The impact of near shading is simulated according to “detailed electrical losses” which is a choice when performing simulation according to electrical losses. Detailed electrical losses represent the sum of the irradiance deficit due to shading and the electrical mismatch of modules in series when the current of a cell is limited due to near shading. Detailed electrical losses accounts for the position of each module and the module layout is defined to correspond table 3.1.

Figure 3.8 illustrates the estimated horizon line in the solar path chart for the PV plant at Campus Evenstad.

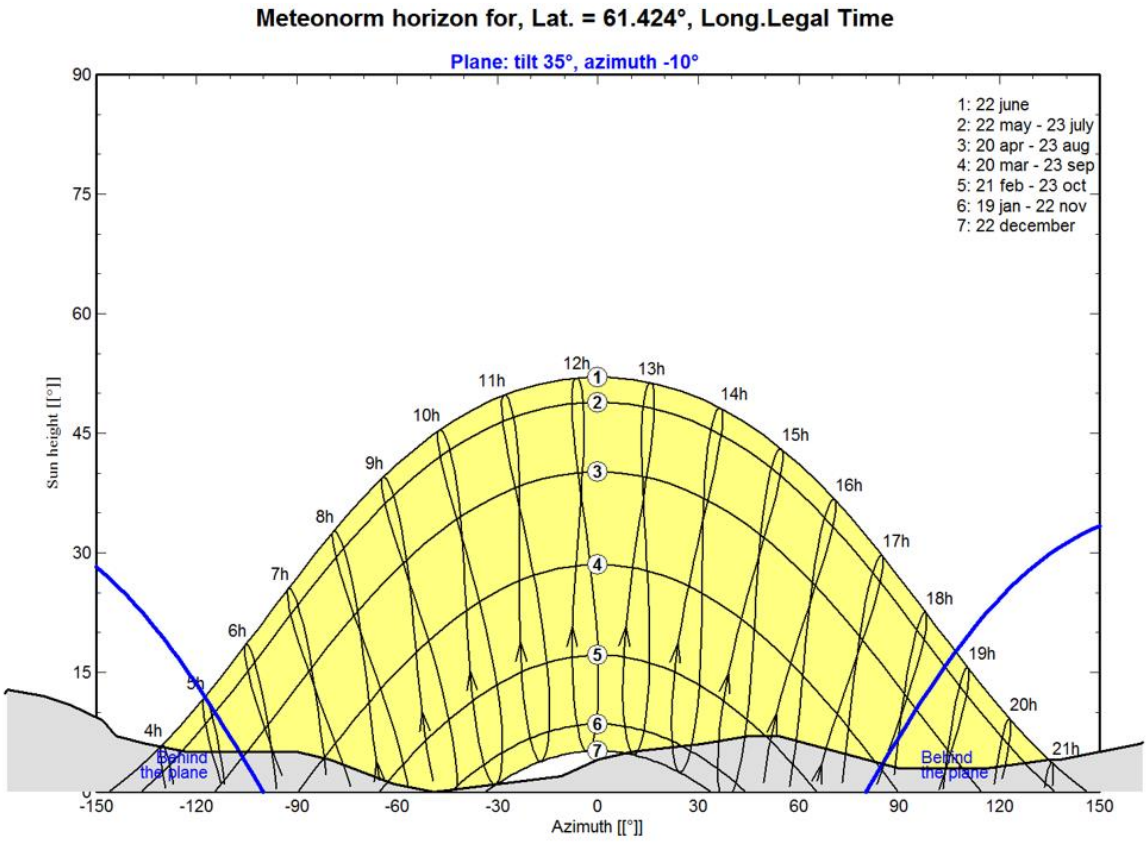

Figure 3.8. Solar path chart made in PVsyst for the PV plant at campus. The chart accounts for the horizontal line, the tilt of the modules and the surface azimuth angle. The grey area illustrates at what time the sun is below the horizontal line and the blue line indicates when the sun moves behind the modules. The x-axis represents the solar azimuth angle and the y-axis represents the solar altitude angle (sun height). PVsyst base the solar chart upon Winter Local Time at Evenstad (UTC+1) for the whole year and the maximum sun height is consequently a few minutes past 12.00. If PVsyst had accounted for Summer Local Time at Evenstad (UTC+2), the maximum sun height would occur a few minutes past 13.00 between end of March and end of October. From PVsyst.

3.2.3 The accuracy of simulations in PVsyst

The simulation accuracy depends on the meteorological data used and the input parameters decided by the user. The interpolated meteorological data used represent an uncertainty in the simulations. Meteorological data should ideally be based upon climatic measurements on site over a long time period instead of interpolated values. PVsyst's implemented values for component's specifications, monthly albedo and loss parameters (except for the IAM values) are kept unchanged. These values in addition to the estimated horizontal line and the estimated dimension and position of shading objects also represent uncertainties in the simulations.

Axaopoulos et al [41] presents results on accuracy test of different simulation software packages, including PVsyst, using climatic data measured on site. It is found that the tested software packages generally underestimate the energy production. The article states that the energy production calculation error results from the PV cell model used by the software package.

3.3 Measured PV production

3.3.1 Measurements

The measured inverter output is displayed in Sunny Portal in intervals of 15 minutes. Every 15-minute value represents the average power output of the previous 15 minutes. Based upon the inverter measurements, the daily, monthly and annual energy production are calculated and displayed in Sunny Portal.

The following measurements are downloaded from Sunny Portal in separate files:

- The power production in 15 min intervals for selected days in the unit kW.
- The daily energy production from March 2017 through September 2017 in the unit kWh.
- The monthly energy production from December 2013 through September 2017 in the unit MWh.

The energy yield measurement error of the inverters is ± 5 % under nominal conditions. [42]

3.3.2 Selection of clear example days

Sunny Portal visualizes the energy production for each day by graphing production profiles. Days with approximately even production profiles are chosen for load match analysis and these days are denoted as clear example days. Table 3.3 shows measured daily yield on selected clear example days.

Table 3.3. The date and the daily energy yield of selected clear example days found in Sunny Portal.

Date	**Measured daily energy yield, kWh**
25.03.2014	430
01.05.2017	498
11.05.2016	510
01.06.2014	527
14.06.2014	527

The sun's path across the horizon at a specific location, and consequently the PV production profiles on clear days, is approximately the same on each side of summer solstice. Selected clear example days therefore represent the date on the other side of summer solstice which is equally many days away from summer solstice.

3.3.3 Selection of cloudy example days

PV production usually vary from day to day due to changing weather conditions. Days with measured energy yield of between 60-70 kWh are selected for load match analysis and are denoted as cloudy example days. Table 3.4 shows the daily energy yield and the energy yield between 07.00 – 17.00 on selected cloudy example days. The time span 07.00 – 17.00 is assumed to be work hours.

Table 3.4. The date and the energy yield of selected cloudy example days found in Sunny Portal. The table displays both the daily yield and the yield between 07:00 – 17:00 which is assumed to be work hours.

Date	Measured daily energy yield, kWh	Measured energy yield between 07:00 and 17:00, kWh
02.04.2016	61.2	52.4
12.04.2014	68.8	50.0
17.04.2014	65.8	58.2
25.04.2015	65.4	58.9
03.05.2016	62.3	53.1
30.05.2015	67.5	56.2

3.4 Analysis of slow charging demand

3.4.1 Measurements and data selection

Measurements
The four slow charging points are measured as a single load on an hourly basis by an energy meter. The energy meter measures the energy supplied to the charging station by the grid. A dataset containing measurements for each day from 16.02.2017 until 13.09.2017 was received from Statsbygg. The received dataset includes both measured energy consumption in kWh for each hour and computer generated average power consumption in kWh/h for each hour.

The energy measurements are only given as integers in kWh. Hourly integer energy measurements have an uncertainty of 0.5 kW if a vehicle is charged constantly at 3.5 kW for an hour and this constitutes an uncertainty of 14 %. The computer generated average power values include decimals. These values reflect better the hourly energy consumption if the vehicles charge constantly at for example 3.5 kW. The computer generated average power values are therefore used in load match analysis instead of the energy measurements.

According to both the energy measurements and the computer generated average power consumption, system losses are between 0.2 – 0.3 kWh/h during hours with no charging demand. According to Salto, the charging station may have idle losses up to 0.15 kWh/h [43]. According to Statsbygg, additional losses may be explained by losses related to connected transformator [37].

Data selection
Following days and time periods were excluded from further study when aiming to find the charging demand during normal operation of the University campus:

- Weekends
- Week 15 due to Easter vacation.
- Days of national holidays
- July due to summer vacation.
- August and September due to less use of the slow charging station because of new charging payment arrangement.

February, March and June were excluded from further study due to measurement errors. The energy consumption of the charging events using computer generated average power values are checked against the energy consumption measured by the energy meter. Two days with charging demand in April and May 2017 were excluded from further study due to energy consumption discrepancy of above 25 %. The energy consumption discrepancy on the 26 remaining days with charging demand was 10 % or less. There were 11 remaining days with charging demand in April 2017 and 15 remaining days with charging demand in May 2017. The demand on each individual day is denoted as a charging profile. The computer generated average power values for each of the 26 remaining charging profiles are given in the Appendix.

3.4.2 Selection of charging profiles

Looking upon the computer generated average power values for April and May 2017, the maximum hourly demand of nine charging profiles was 3.5 – 3.8 kWh/h, the maximum hourly demand of eight charging profiles was 6.8 – 8.3 kWh/h and the maximum hourly demand of nine charging profiles was 10.1 – 13.8 kW/h. Charging profiles were divided into three groups according to the maximum hourly demand. One charging profile from each group was selected for load match analysis. The selected charging profiles aim to describe different characteristics of the charging demand at campus.

Since the charging demand at campus is measured as a single load, the number of vehicles charging simultaneously is unknown. Assumptions regarding the charging power and the number of vehicles charging are decided based upon the slow charging curve presented in figure 2.8.

Figure 3.9 shows the maximum hourly demand of each charging profile in April and May 2017.

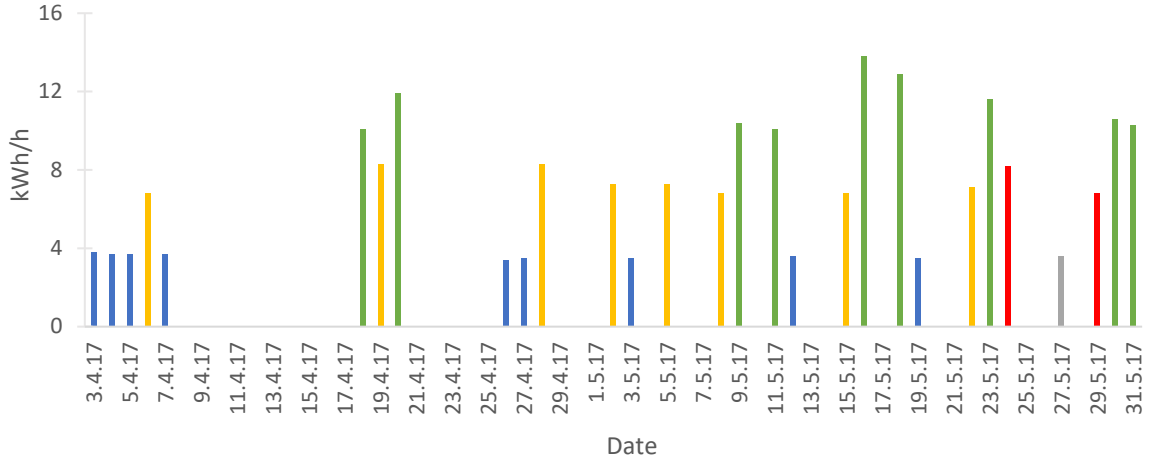

Figure 3.9. The date and maximum hourly demand of charging profiles in April and May 2017. The different colours represent different groups of charging profiles. Blue represents charging profiles with maximum hourly demand of 3.5 – 3.8 kWh/h, yellow represents charging profiles with maximum hourly demand of 6.8 – 8.3 kWh/h, green represents charging profiles with maximum hourly demand of 10.1 – 13.8 kWh/h, grey represents charging profiles within weekends and red represents charging profiles excluded from load match analysis due to energy discrepancy between energy measurements and computer generated average power consumption.

3.5 Analysis of fast charging demand

Charging data which shows the use of ABB's charging station was received by ABB. The dataset contained:

- Date
- Charging connector number
- Charging start-time
- Charging duration in minutes
- Amount of energy transferred to the connector in kWh
- Charging stop-reason being either "stopped by vehicle", "stopped by user" or "stopped remotely"

Each connector is measured separately and the charging data covered 9 months extending from 07.11.2016 – 03.09.2017. The dataset lists 111 charging events during this time.

The fast charging data are used to study the time distribution of fast charging events at Campus Evenstad in addition to study the energy demand and the mean power demand of the events.

3.6 Charging scenarios

As mentioned in chapter 2, the EV fleet in Norway is increasing. In accordance to this development, different scenarios are made which presuppose an increased number of available connectors at campus facilitating an increased charging demand. There are 70 employees working at Campus today and the different scenarios define different percentages of employees charging their car daily at work. In addition, the scenarios are based on following assumptions:

- The net energy capacity of EVs charging are 21.6 kWh corresponding to the most sold car today (Nissan Leaf).
- 89 % of the power drawn from the grid is taken up by the battery and the vehicles charge 50 % of net energy capacity.
- Each vehicle charge at 3.5 kW.
- The demand of the vehicles is distributed over eight hours between 08:00 – 16:00 so that the total power demand is the total energy demand divided by eight hours.

Number of cars charging and the daily energy demand of each scenario are given in table 3.5.

Table 3.5. The number of cars charging daily and the corresponding energy demand according to scenario assumptions.

Scenarios	**Number of cars charging**	**Total energy demand, kWh**
Scenario 1: 10% of employees	7	85
Scenario 2: 20% of employees	14	170
Scenario 3: 30% of employees	21	255

3.7 Load match analysis

3.7.1 PV production and selected charging profiles

The selected charging profiles discussed in chapter 3.4.2 are used to decide and/or discuss load match between EV demand at the slow charging station and measured PV production on clear and cloudy example days. The load match factors self consumption and self generation are calculated on an hourly basis using formulas 2.4 and 2.5. Load match between selected charging profiles and PVsyst simulated production profiles of clear days are also discussed.

In addition, the daily PV production and the total demand of the selected charging profiles are compared. PVsyst simulation of a typical year are used to decide the percentage of days which may supply the daily demand of the selected charging profiles from February through November.

3.7.2 PV production and charging scenarios

The same method is used when studying load match between the scenario demand discussed in chapter 3.6 and PV production as when studying load match between the selected charging profiles and PV production (which was described in chapter 3.7.1).

3.7.3 PV production and fast charging

Load match between fast charging demand and PV production is studied using ABB's demand measurements, production measurements of clear days and PVsyst simulated production on clear days.

4. Results

Chapter 4.1 looks upon how the PVsyst simulations correspond to measured production and shows different uncertainties regarding the simulations so that the simulation results may be interpreted accordingly. Chapter 4.2 presents PVsyst simulated clear day production profiles throughout the year, while chapter 4.3 summarizes the charging demand at the slow charging station and the fast charging station at Campus Evenstad. Chapter 4.4 investigates the load match between the slow charging demand, the fast charging demand, the production on measured example days and the production according to PVsyst simulations.

4.1 Comparison of simulated PV production and measured PV production

4.1.1 Typical year simulation

Figure 4.1 compares the simulated monthly production in a typical year, the measured monthly production from December 2013 through September 2017 and the measured production mean for each month. The figure shows that:

- The simulated production exceeds the measured production in January, March and December 2013-2017.
- The measured production in August 2013-2017 exceeds the simulated production for August.
- The simulated production is in between the measured monthly production for February, April, May, June, July, September, October and November 2013-2017.

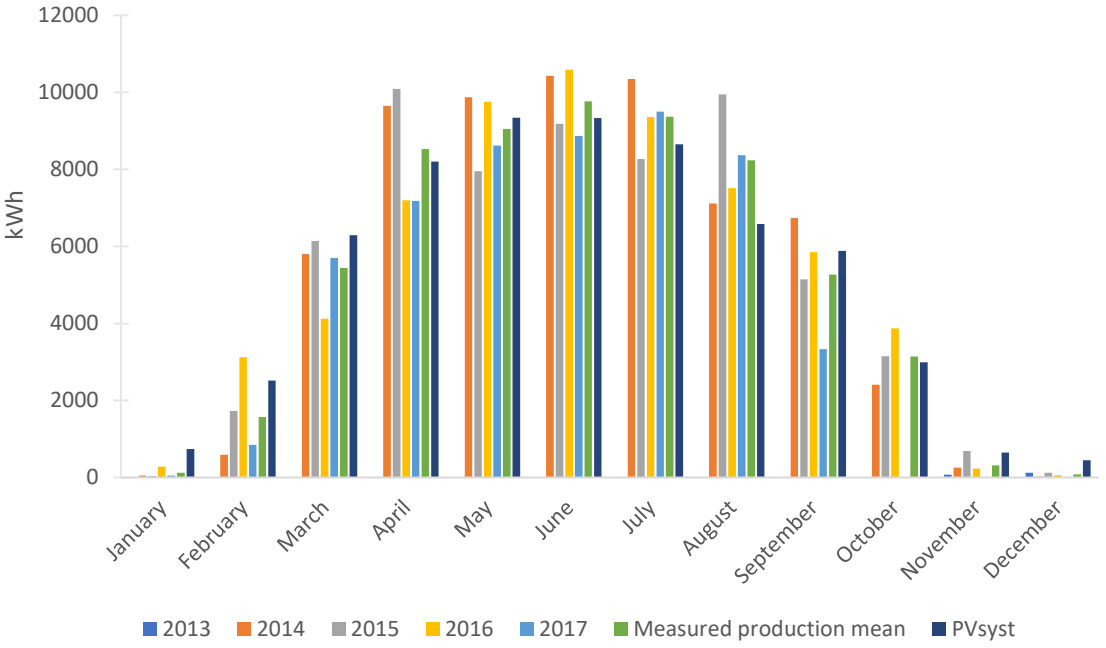

Figure 4.1. PVsyst simulated monthly production for a typical year, the measured production for each month from December 2013 through September 2017 and the measured production mean.

Table 4.1 shows the mean and the standard deviation of measured production. The large standard deviation for some months shows that the monthly production varies to a large extent from year to year due to weather conditions. The standard deviation is especially large for January, February, November and December where the standard deviation is between 60 – 95%.

Table 4.1 also shows the monthly production according to the PVsyst simulation of a typical year. The simulated production for December and January is about five times as large as the monthly mean of measured production. This may indicate that PVsyst overestimate production during these months. Overestimated production may be caused by inaccurate meteorological data for these months or snow-covered modules.

Note that the measured production mean is statistically invalid to define the typical monthly production at Campus Evenstad since the PV plant has only been operative for four years.

Table 4.1. The monthly mean, the annual mean and the standard deviation of measured production in addition to the PVsyst simulated monthly and annual production.

Month	**Measured monthly mean and standard deviation, $\mu \pm \sigma$, kWh**	**PVsyst simulation, kWh**
January	123 ± 117	741
February	1573 ± 1141	2515
March	5440 ± 900	6287
April	8530 ± 1558	8203
May	9050 ± 926	9342
June	9768 ± 869	9336
July	9370 ± 854	8648
August	8235 ± 1258	6584
September	5266 ± 1252	5883
October	3143 ± 730	2994
November	313 ± 265	649
December	80 ± 49	444
Year	62370 ± 803	61626

The typical year simulation is used for load match analysis in chapters 4.4.3 and 4.4.5 to present an idea of percentages of days in February through November which has a certain energy yield in a typical year. December and January are excluded from load match analysis due to low energy expectancy.

4.1.2 Clear day simulation

The daily yield and the production profile on the clear example days are compared to the PVsyst simulated production. Table 4.2 compares the measured daily yield with the simulated daily yield. In each case, the daily yield is underestimated by PVsyst and the difference is up to 8.8%.

Table 4.2. Comparison of measured production on clear example days and PVsyst simulated clear day production.

Date	**Measured yield, E_m, kWh**	**Simulated yield, E_s, KWh**	**Difference, $E_m - E_s$, kWh**	**Difference, %**
25.03.2014	430	392	38	8.8
01.05.2017	498	477	21	4.2
11.05.2016	510	491	19	3.7
01.06.2014	527	503	24	4.6
14.06.2014	527	510	17	3.2

Figure 4.2 compares simulated production for 01.05 and the measured production on 01.05.2017. The figure illustrates that PVsyst underestimates the production during production peak hours. In a 15 minutes interval, the average peak power production was 59 – 60 kW on clear example days. The simulated power peak production for the same dates was 54 kW – 55 kW. In addition, the PVsyst simulation slightly overestimate the production in the morning and slightly underestimate the production in the afternoon/evening. The same discrepancy between measured production and simulated production is seen for every clear example day.

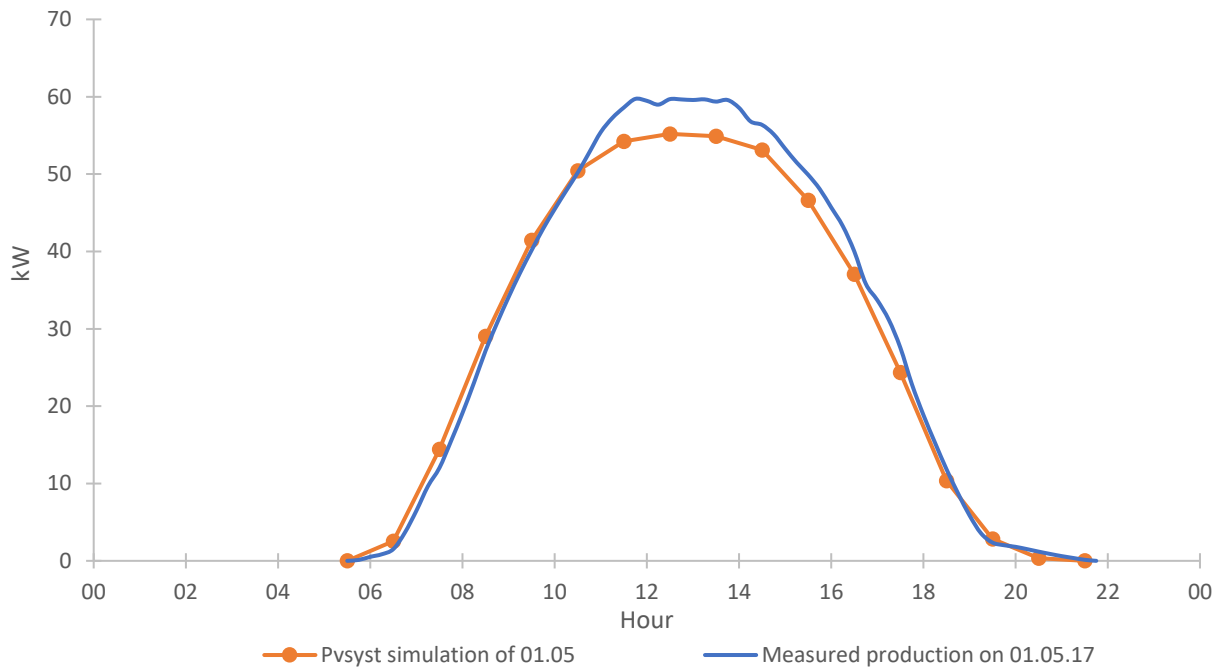

Figure 4.2. Measured production on 01.05.2017 and PVsyst simulated production for 01.05.

4.2 Simulated production profiles of clear days throughout the year

Figure 4.3a-b shows simulated clear day production profiles from 01.02 until 08.11. Each profile is based on simulated instantaneous power values which are given every thirty minutes past full hour. The production profiles are in two-weeks interval starting on 21.06 (summer solstice). The profiles between 27.10 – 28.03 are graphed according to UTC+1 and the profiles between 29.03 – 27.10 are graphed according to UTC+2. Local time shift from UTC+1 to UTC+2 leads to a time shift in production peak from around 12:00 to around 13:00.

The production profiles in figure 4.3a are denoted spring profiles and the production profiles in figure 4.3b are denoted autumn profiles. The power values of each profile are given in Appendix.

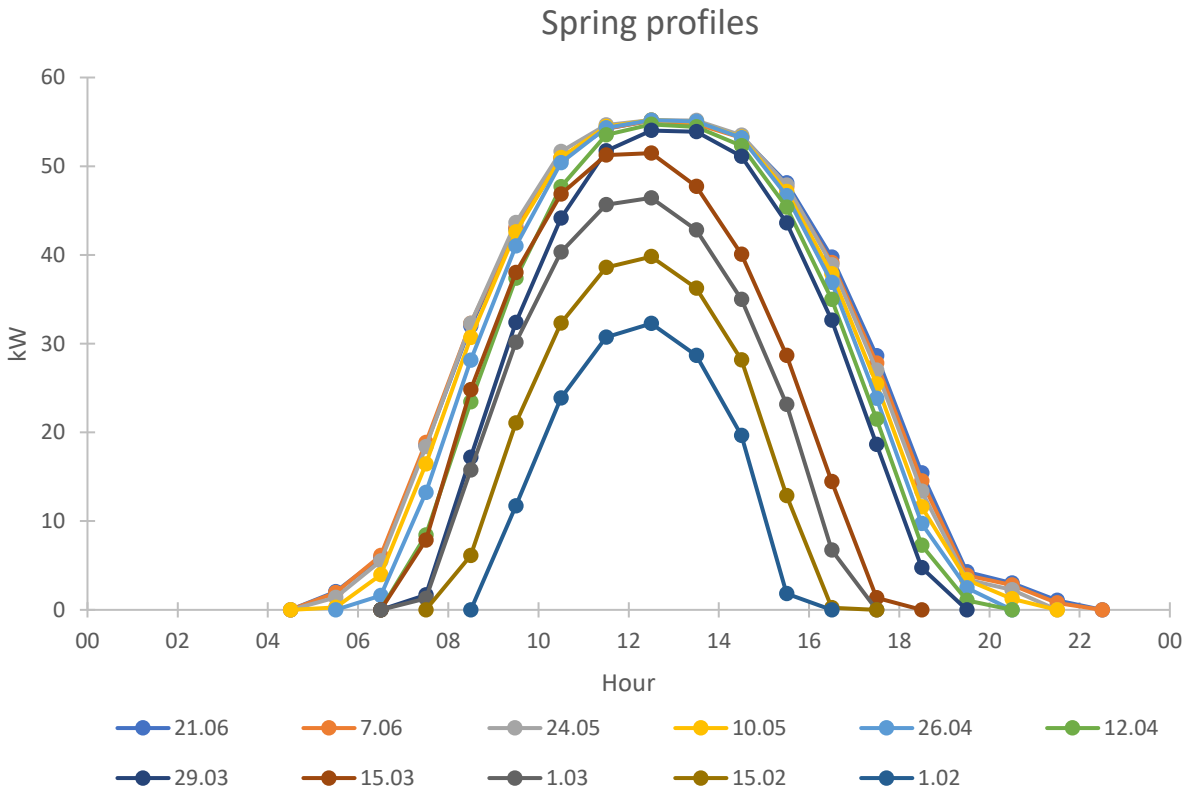

Figure 4.3a. PVsyst simulated production profiles in two-weeks intervals between 01.02 – 21.06.

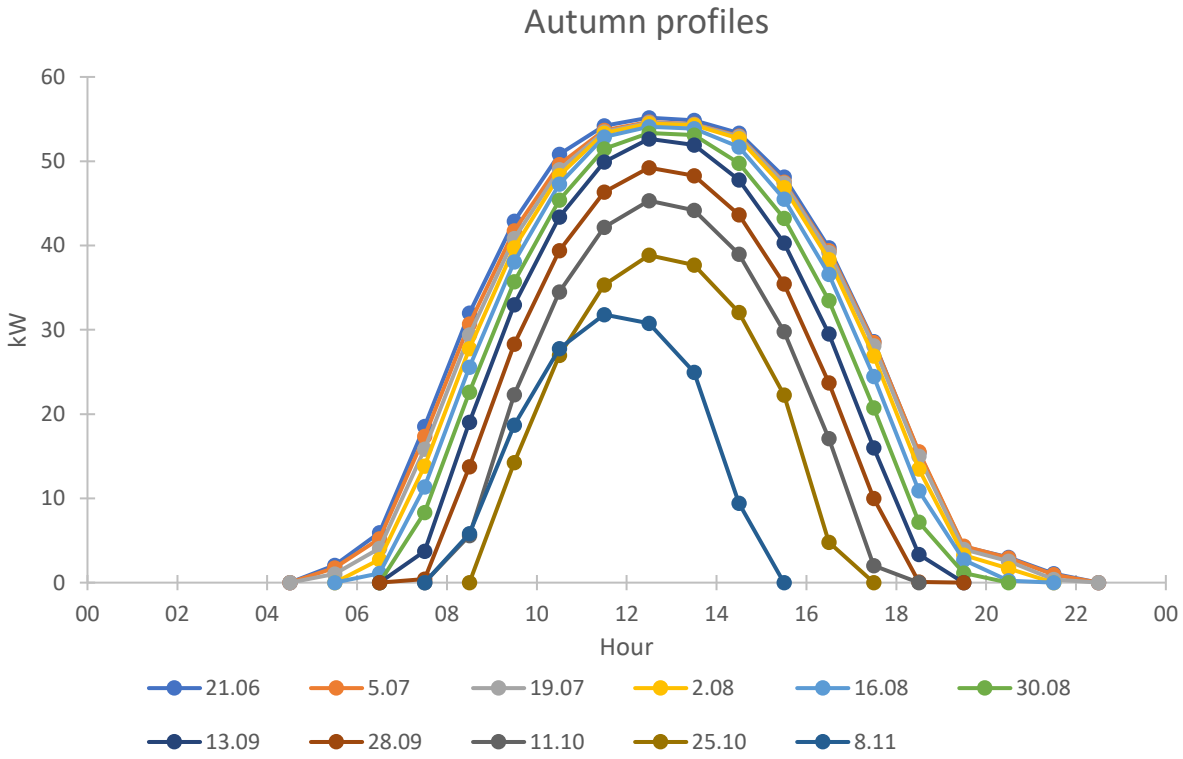

Figure 4.3b. PVsyst simulated production profiles in two-weeks intervals between 21.06 – 08.11.

Studying the profiles in figure 4.3a-b, it seems that the production is only impacted by shading at the start and at the end of production hours. According to the PVsyst simulation, the annual loss due to far shading is 2.1% and these losses occur at the start of production hours and towards the end of production hours. The trees may cast shadow on the PV array, but over the year, the shading losses due to near shading are 0.0 % according to the PVsyst simulation.

Figure 4.3a-b shows how the clear day production profile changes relative to the clear day production profile two-weeks before or two-weeks after. Relative to each other, the production profiles change the least during weeks close to summer solstice. When comparing the simulated production profiles on dates which are equally many days away from summer solstice, it is found that the spring profiles have a higher production, between 0.1 – 3 kW, during morning hours and peak hours than the corresponding autumn profiles. The autumn profiles have a higher production during evening hours, between 0.1 – 1.5 kW, compared to the spring profiles. This production discrepancy between profile-pairs is illustrated in figure 4.4 which shows the simulated production profiles for 26.04 and 16.08.

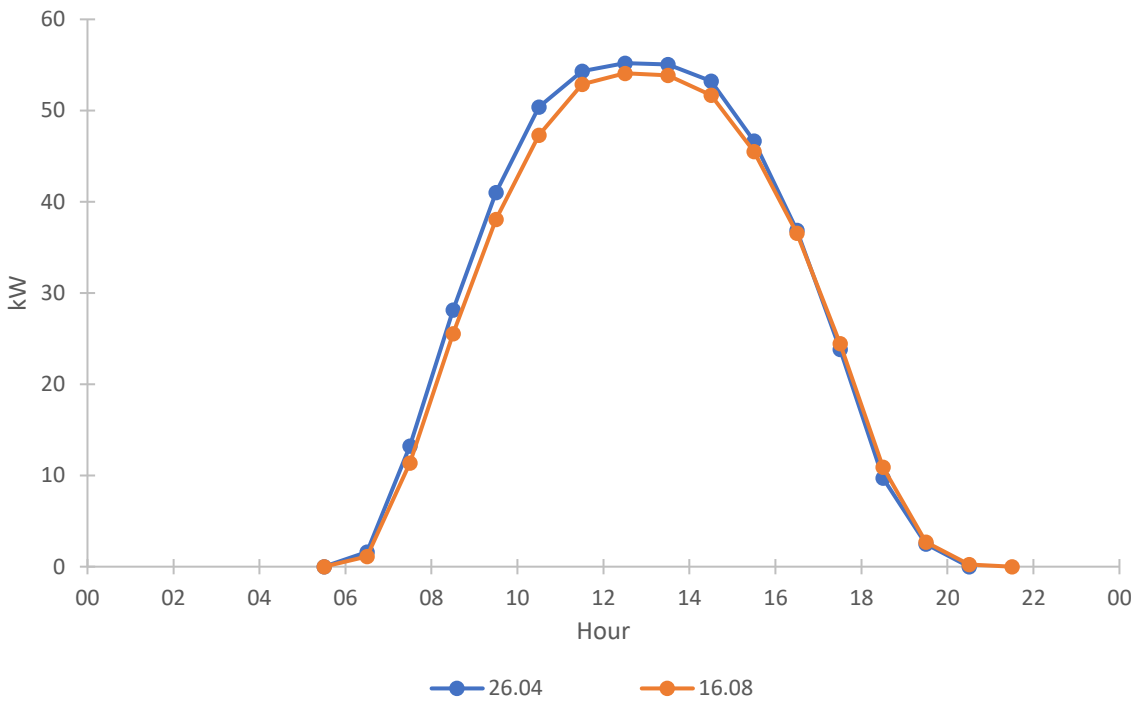

Figure 4.4. Simulated clear day production profiles for 26.04 and 16.08.

Table 4.3 shows the energy yield of the production profiles in figure 4.3a-b. The simulated energy yield on clear days may be underestimated as seen when comparing measured production on clear example days and PVsyst simulated production in table 4.2. Table 4.3 merely aims to compare the simulated energy yield on clear days on each side of summer solstice. The greatest difference in energy yield between production profile-pairs is 4%.

Table 4.3. Energy yield of simulated clear day production profiles in two weeks interval between 01.02 and 08.11. The energy yield on dates which are equally many days away from summer solstice is close to the same.

Date (spring)	**Simulated energy yield, kWh**	**Date (autumn)**	**Simulated energy yield, kWh**
21.06	510.1	**21.06**	510.1
07.06	507.0	**05.07**	501.2
24.05	504.2	**19.07**	492.1
10.05	489.5	**02.08**	477.7
26.04	471.8	**16.08**	456.3
12.04	442.0	**30.08**	425.5
29.03	405.7	**13.09**	390.6
15.03	352.5	**28.09**	338.7
01.03	287.3	**11.10**	281.9
15.02	215.4	**25.10**	212.2
01.02	148.7	**08.11**	149.2

The simulated production profiles illustrated in figure 4.3a-b are used in chapters 4.4.1, 4.4.2, 4.4.4 and 4.4.6 to give an idea of the clear day production at Evenstad in the morning and in the afternoon/evening.

4.3 Charging demand at campus

4.3.1 Slow charging

The slow charging station was mainly used in the morning in week days according to measurements in April and May 2017. There were altogether 29 days with charging demand during these two months. Only one of these days was within a weekend and this charging event was the only one occurring in the evening. None of the charging events occurred on a national holiday and none during Easter week (week 15). The charging station was used between 3 to 5 days per week, typically 3 days. The measurements in April and May 2017 therefore suggest that the charging demand at campus is mainly work charging demand by employees at the University.

As mentioned in chapter 3.4.2, the charging profiles were divided into three groups according to maximum hourly demand. Different characteristics of the charging demand in each group are described below.

Maximum hourly demand: 3.5 – 3.8 kWh/h

Most of the charging profiles which had a maximum hourly demand of 3.5 – 3.8 kWh/h started between 07:00 and 08:00. The charging demand typically lasted for 4 – 6 hours and the total energy consumption was typically between 11.7 – 12.6 kWh. The charging demand on 12.05.17 is selected for load match analysis and is denoted “charging profile 1”. Table 4.4 and figure 4.5 lists and illustrates the hourly demand of charging profile 1.

Charging profile 1 is assumed to represent the demand of one vehicle. The vehicle started to charge at 3.5 kW at around 07:30. As the vehicle approached full capacity, the charging power started to gradually decrease sometime between 10:00 and 11:00. The charging ended sometime between 11:00 and 12:00. A representation of this charging curve is shown in figure 4.6.

Maximum hourly demand: 6.8 – 8.3 kWh/h

Most of the charging profiles which had a maximum hourly demand of 6.8 – 8.3 kW started between 07:00 and 08:00. The demand typically lasted for 4 – 7 hours and the total energy consumption was usually 20 – 30 kWh. The charging demand on 22.05.17 is selected for load match analysis and is denoted “charging profile 2”. Table 4.4 and figure 4.5 lists and illustrates the hourly demand of charging profile 2.

Charging profile 2 is assumed to represent the demand of two vehicles. Each vehicle started to charge at 3.5 kW at around 07:30. As the vehicles approached full capacity, the charging power started to gradually decrease sometime between 10:00 and 11:00. The charging ended sometime between 11:00 and 12:00.

Maximum hourly demand: 10.1 – 13.8 kWh/h

Most of the charging profiles which had a maximum hourly demand of 10.1 – 13.8 kW started between 07:00 and 08:00. The demand lasted between 6 – 10 hours and the total energy consumption was above 40 kWh on most days. The charging demand on 18.05.17 is selected

for load match analysis and is denoted “charging profile 3”. Table 4.4 and figure 4.5 lists and illustrates the hourly demand of charging profile 3.

Although it is challenging to make assumptions regarding the number of vehicles charging in charging profile 3, the load match of this charging profile is studied in the same way as for charging profile 1 and charging profile 2.

Table 4.4. The computer generated average power values of the selected charging profiles. Charging profile 1 is the charging demand on 12.05.2017. Charging profile 2 is the charging demand on 22.05.2017. Charging profile 3 is the charging demand on 18.05.2017.

	Charging profile 1, kWh/h	**Charging profile 2, kWh/h**	**Charging profile 3, kWh/h**
07:00 – 08:00	1.9	3.7	3.6
08:00 – 09:00	3.6	7.1	10.6
09:00 – 10:00	3.6	7.1	12.9
10:00 – 11:00	2.0	4.8	8.2
11:00 – 12:00	0.7	1.3	4.2
12:00 – 13:00	-	-	3.6
13:00 – 14:00	-	-	2.4

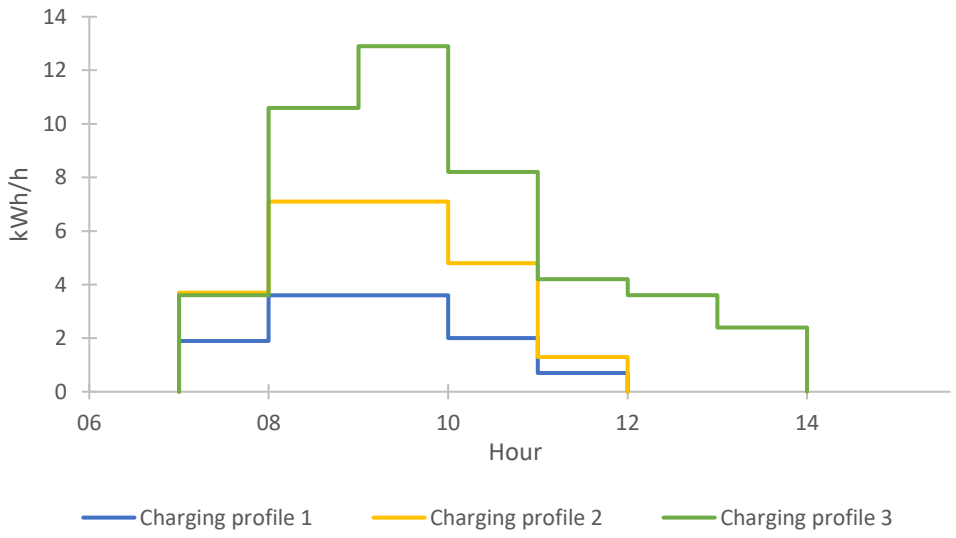

Figure 4.5. The hourly demand of the selected charging profiles.

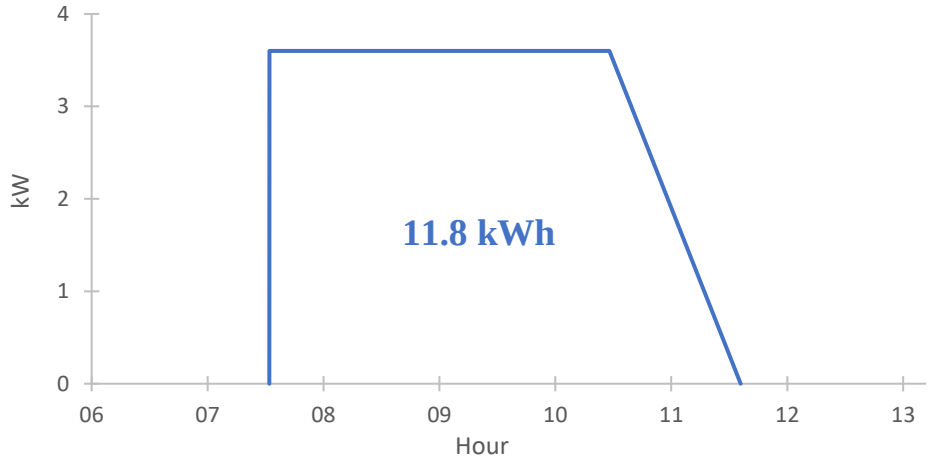

Figure 4.6. A representation of assumed charging curve for charging profile 1.

The total energy demand of charging profile 1, charging profile 2 and charging profile 3 is given in table 4.5.

Table 4.5. The total energy demand of the selected charging profiles.

	Charging profile 1	**Charging profile 2**	**Charging profile 3**
Energy demand, kWh	11.8	24.0	45.5

4.3.2 Fast charging

Between 7.11.2016 – 3.9.2017, there were 111 charging events at the charging station which was delivered by ABB. DC power were used for 106 charging events and AC power were used for 5 charging events. Figure 4.7 shows at what time the charging events occurred where the number of charging events on each hour represents the number of charging events which occurred in the previous hour. The figure shows that the fast charging events was distributed throughout the day, but most events occurred between 13:00 and 16:00.

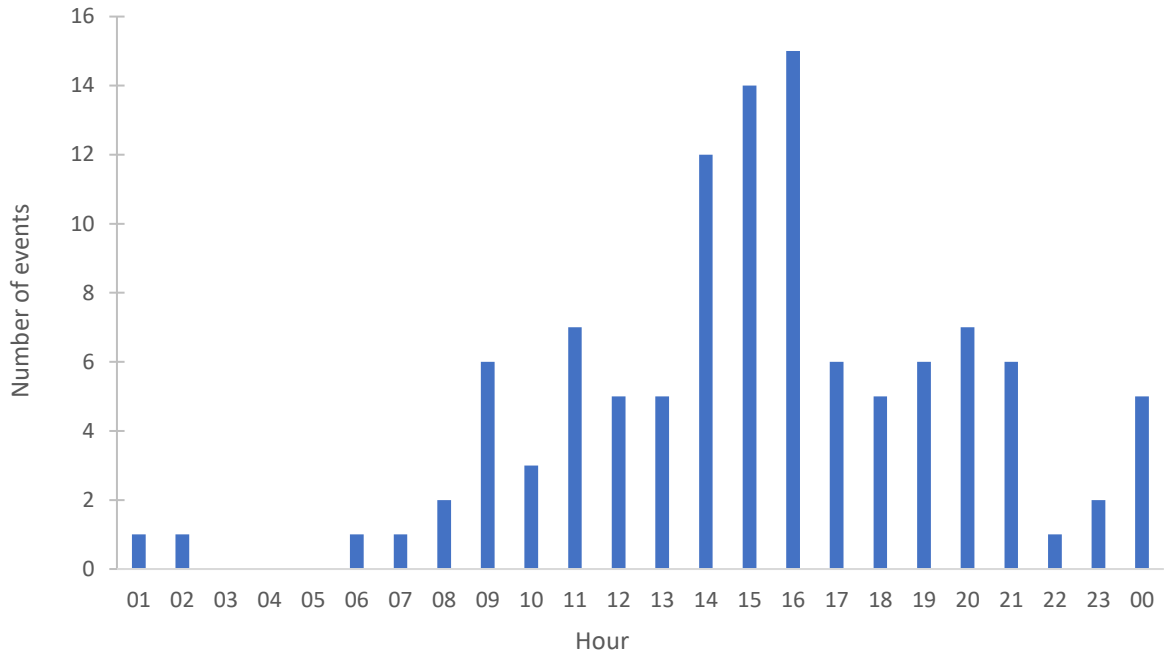

Figure 4.7. The distribution of fast charging events throughout the day according to measurements from ABB's station between 7.11.2016 – 3.9.2017. The number of charging events for each hour represents the number of charging events which occurred in the previous hour.

Figure 4.8 and figure 4.9 show the duration, the mean charging power and the energy consumption of the charging events which used DC power.

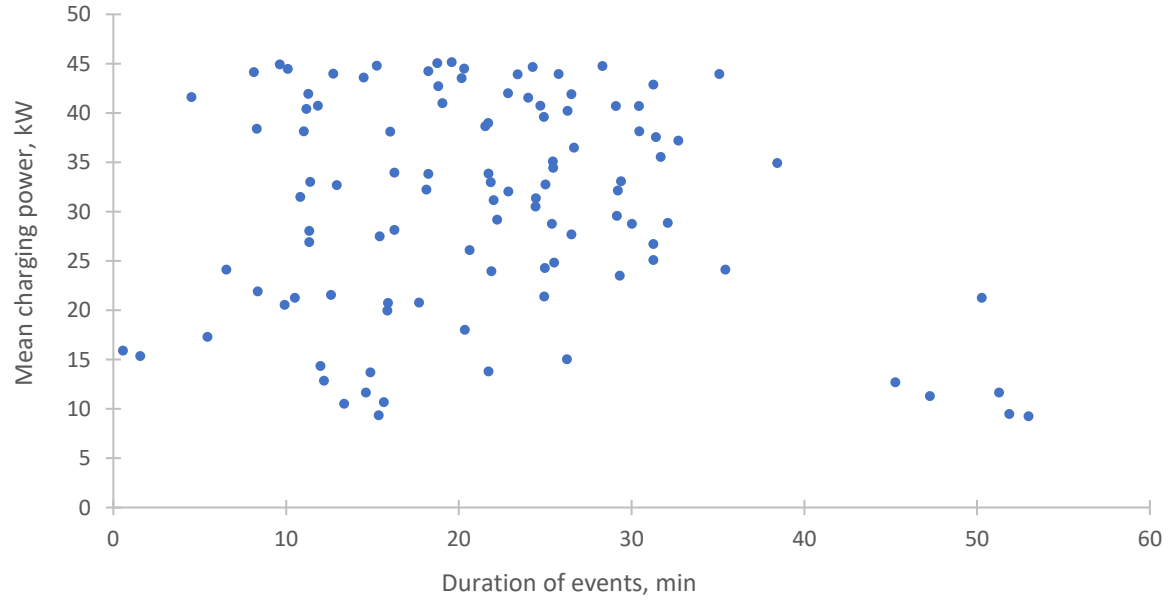

Figure 4.8. The mean charging power and the duration of the charging events which used DC power at ABB's station between 7.11.2016 – 3.9.2017.

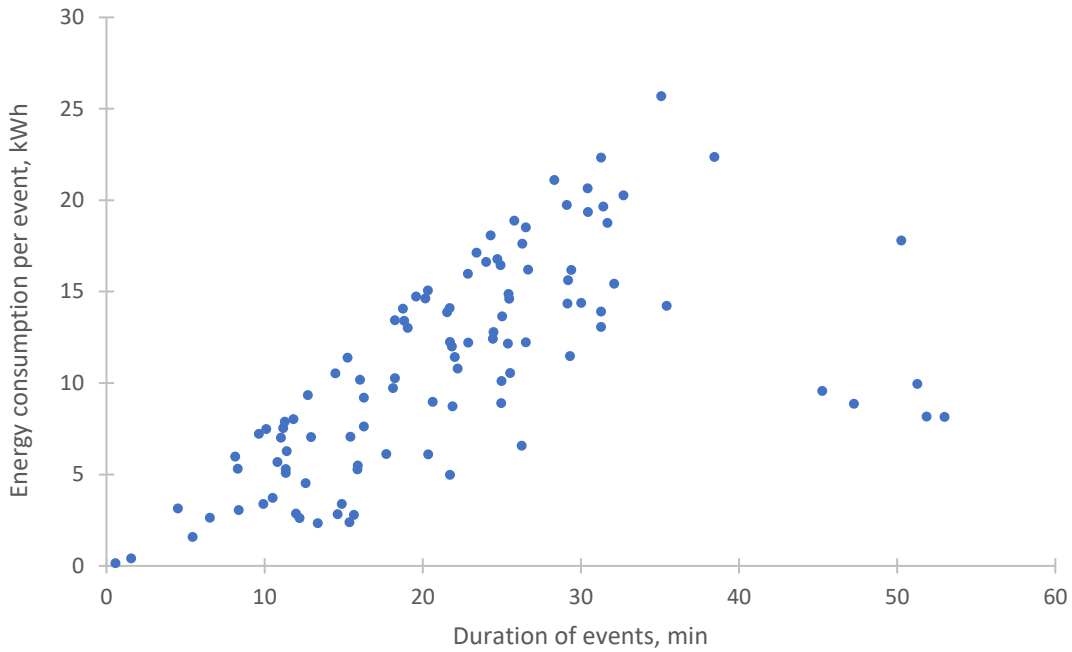

Figure 4.9. The energy consumption and the duration of each charging events which used DC power at ABB's station between 7.11.2016 – 3.9.2017.

Figure 4.8 and 4.9 show that most charging events lasted for less than 35 minutes and that the maximum mean power and the maximum energy demand were 45 kW and 26 kWh respectively.

4.4 Load match analysis

4.4.1 Load match potential

The simulated instantaneous power value at 07:30 and 08:30 of each clear day simulated spring profile is given in table 4.6. Table 4.6 depicts the maximum number of EVs which may charge at 3.5 kW using only photovoltaic power at 07:30 and 08:30 if losses in the charging system are neglected. The table shows that the longer the charging demand is postponed in the morning on clear days, the more EVs may be supplied by PV power exclusively for a larger portion of the year.

A similar table can be made for each clear day simulated autumn profile. As already seen, the morning production of autumn profiles are slightly lower than the morning production of corresponding spring profiles. Consequently, the maximum number of vehicles charging using only photovoltaic power at 07:30 and 08:30 may be lower.

Table 4.6. Number of EVs charging at 3.5 kW using only locally produced PV power at 7.30 and 8.30 based upon simulated clear day production profiles. The decrease in power production on 29.03 compared to 15.03 is the result of local time shift from UTC+1 to UTC+2.

Date	PV power production at 07:30 / 08:30	Possible number of EVs charging at 07:30	Possible number of EVs charging at 08:30
21.06	19 kW / 32 kW	5	9
07.06	19 kW / 32 kW	5	9
24.05	18 kW / 32 kW	5	9
10.05	16 kW / 31 kW	4	8
26.04	13 kW / 28 kW	3	8
12.04	8.4 kW / 23 kW	2	6
29.03	1.8 kW / 17 kW	0	4
15.03	7.9 kW / 25 kW	2	7
01.03	1.3 kW / 16 kW	0	4
15.02	0.0 kW / 6.1 kW	0	1
01.02	0.0 kW / 0.0 kW	0	0

4.4.2 PV production and selected charging profiles on clear days

Figure 4.10 shows the daily energy balance between the energy production on clear example day 01.05.2017 and the selected charging profiles. In general, the energy production on clear example days exceeds the demand of the selected charging profiles by 400 - 500 kWh.

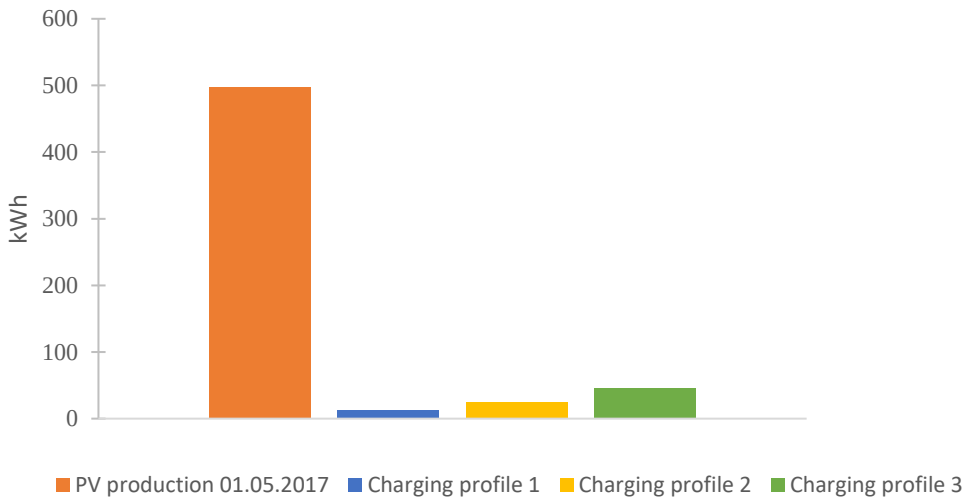

Figure 4.10. Energy balance between PV production on 01.05.20157 and the demand of the selected charging profiles.

Every clear example day produced sufficient energy to supply the hourly demand of each of the selected charging profiles. In general, the self generation factor equalled 1. The hourly self consumption factors are listed in table 4.7. The self consumption range represents the range of values found for different example days. The minimum value represents either example day 25.03.2014 or 14.06.2014 and the maximum value represents example day 01.05.2017. The production on 25.03.2014 is the only clear example day which is measured according to

UTC+1 instead of UTC+2. This explains the large production and the low self consumption values during morning hours compared to other clear example days which are closer to summer solstice.

Table 4.7 shows that the demand of the selected charging profiles covered less than 40 % of the hourly production in the morning and less than 10 % of the hourly PV production around midday on clear example days.

Table 4.7. Self consumption range of the demand of selected charging profiles on clear example days.

	Charging profile 1	**Charging profile 2**	**Charging profile 3**
07.00 – 08.00	0.11 – 0.14	0.21 – 0.26	0.20 – 0.26
08.00 – 09.00	0.11 – 0.13	0.21 – 0.25	0.32 – 0.37
09.00 – 10.00	0.08 – 0.09	0.15 – 0.17	0.28 – 0.31
10.00 – 11.00	0.04	0.09	0.16
11.00 – 12.00	0.01	0.02	0.07
12.00 – 13.00	-	-	0.06
13.00 – 14.00	-	-	0.04

The PVsyst simulation of clear days throughout the year is used to investigate how time of year impacts the hourly load match. As already mentioned, the simulated profiles are based on simulated power values given every thirty minutes past a full hour. Deciding hourly load match is therefore challenging. Assuming that linear lines between each given power value represent the instantaneous power increase/decrease throughout the day, it seems that the hourly production on 15.03 until 13.09 is sufficient to supply the hourly demand of each selected charging profile. Figure 4.11 illustrates the hourly demand of the charging profiles and simulated PV production profiles in February and March.

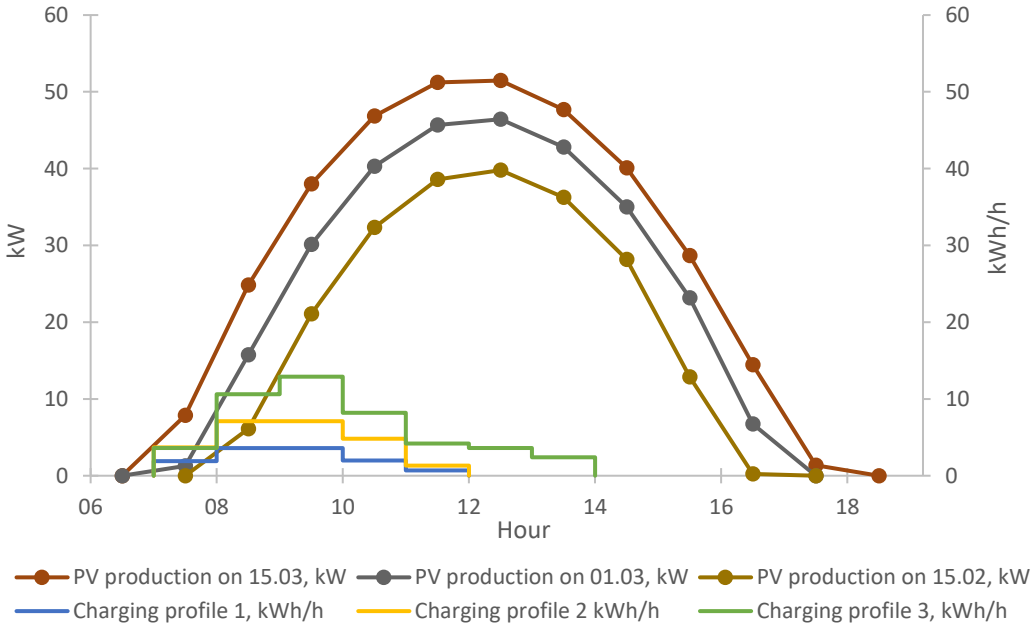

Figure 4.11. The hourly demand of selected charging profiles and simulated clear day production profiles in February and March.

4.4.3 PV production and selected charging profiles on cloudy days

Figure 4.12 shows the daily energy yield in March through September 2017. The figure illustrates that the PV production vary from day to day due to changing weather conditions. Figure 4.13 shows the measured production on 03.05.2016, which is one of the selected cloudy example days.

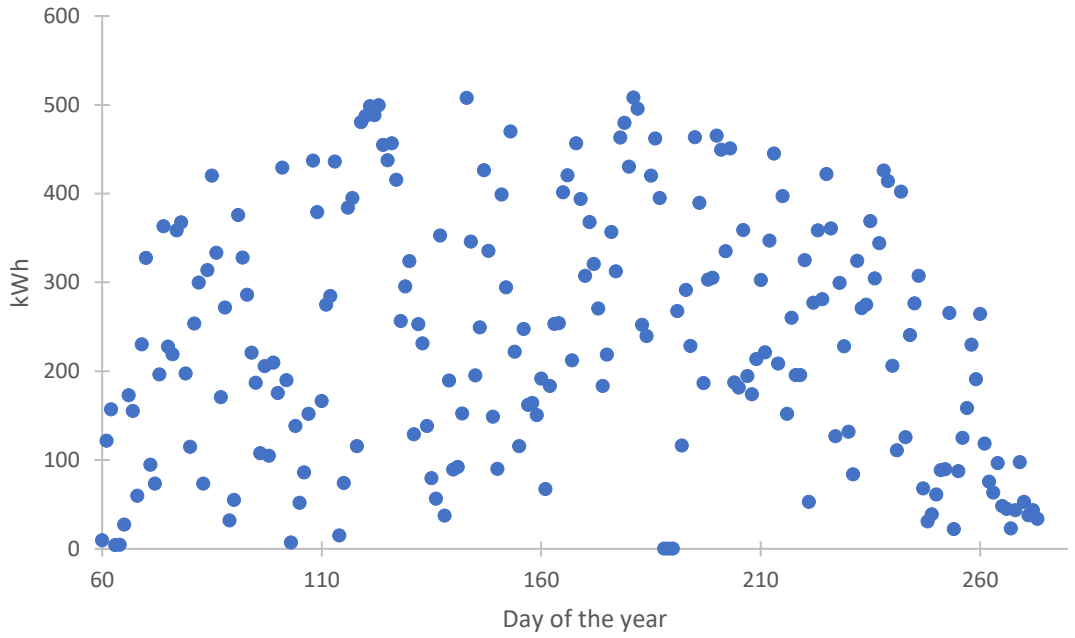

Figure 4.12. The measured PV yield of each day in March through September 2017.

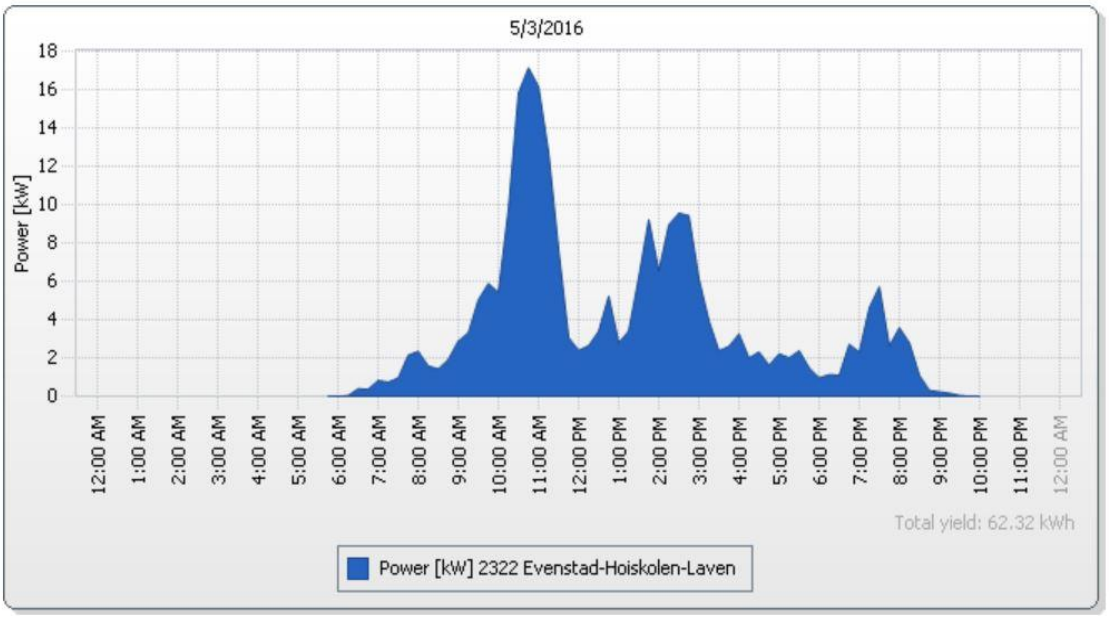

Figure 4.13. PV production on 03.05.2016 as presented in Sunny Portal.

The energy produced on cloudy example days exceeds the demand of the selected charging profiles, but the hourly load match factors vary depending on the amount of cloud coverage during demand hours. The production on example day 30.05.2015 can supply charging profile 1 hourly, but is insufficient to supply the hourly demand of charging profile 2 and charging profile 3. The production on each of the other cloudy example days is insufficient to supply any of the selected charging profiles on an hourly basis. In these cases, a charging system which adjust the charging power according to the power production is necessary to ensure that the demand is covered on an hourly basis by locally produced PV production.

Table 4.8. shows the percentage of days in February through November where the daily production exceeded the demand of the charging profiles according to PVsyst simulation of a typical year.

Table 4.8. The percentage of days where the daily energy yield in each month exceeded 11.8 kWh, 24.0 kWh and 45.5 kWh according to PVsyst simulation of a typical year.

	≥ 11.8 kWh	**≥ 24.0 kWh**	**≥ 45.5 kWh**
February, %	86	79	61
March, %	100	97	97
April, %	100	100	100
May, %	100	100	100
June, %	100	100	97
July, %	100	100	100
August, %	100	100	100
September, %	100	100	93
October, %	84	52	45
November, %	50	33	13

Table 4.8 shows that the daily production exceeds the daily demand of the selected charging profiles on more than 98% of the days in March through September. Out of the months listed in table 4.8, only November showed a daily coverage of 50% or less for each charging profile. Note that the percentages of daily coverage change if the charging demand is increased which likely is the case during winter months.

4.4.4 PV production and scenario demand on clear days

As described in chapter 3.6, the scenarios assume that 7, 14 and 21 vehicles charge daily at campus. The energy production on clear example days exceeds the demand of scenario 1 by 350 – 440 kWh, the demand of scenario 2 by 260 – 360 kWh and the demand of scenario 3 by 180 – 270 kWh. Figure 4.14 illustrates the energy balance between the scenario demands and the energy production on clear example day 01.05.17.

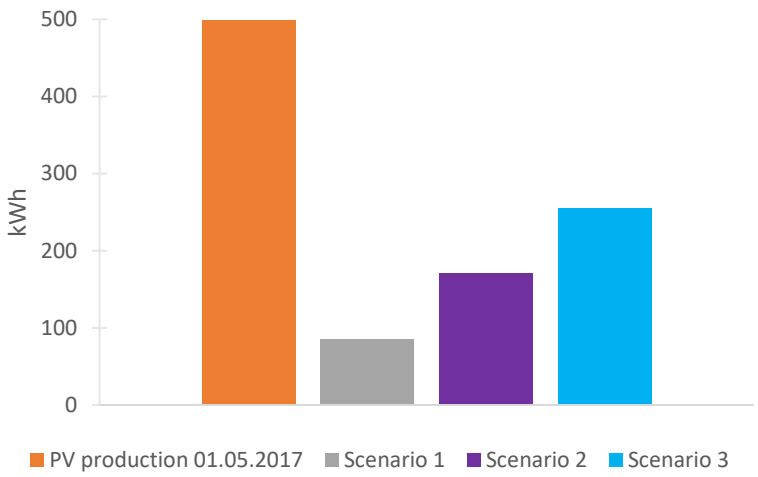

Figure 4.14. Energy balance between PV production on 01.05.2017 and scenario demand.

Each clear example day produced sufficient energy to supply the hourly demand of scenario 1 and scenario 2. The self generation factor in these cases equalled 1. Only example day 25.03.2014 and 14.06.2014 produced sufficient energy to supply the hourly demand of scenario 3 between 08:00 and 09:00. The deficit energy on the remaining clear example days was at most 3.2 kWh and the self generation factor ranged between 0.90 – 1.0. For the remaining hours, 09:00 – 16:00, the production on every clear example day was sufficient to supply the hourly demand of scenario 3 and the self generation equalled 1.

The self consumption range in table 4.9 represents the range of values found for the clear example days which are measured according to UTC+2. The minimum value represents example day 14.06.2014 and the maximum value represents example day 01.05.2017. Note that the clear example days which follow UTC+2 produce sufficient hourly energy to supply the demand of 21 vehicles if the charging demand is set to last between 09:00 – 17:00 instead of lasting between 08:00 – 16:00.

Table 4.9. Self consumption range of scenario demand and production on 01.05.2017, 11.05.2016, 01.06.2014 and 14.06.2017.

	Scenario 1	**Scenario 2**	**Scenario 3**
08.00 – 09.00	0.33 – 0.37	0.66 – 0.74	0.99 – 1.0
09:00 – 10:00	0.24 – 0.26	0.48 – 0.51	0.73 – 0.77
10:00 – 11:00	0.20 – 0.21	0.40 – 0.41	0.60 – 0.62
11:00 – 12:00	0.18 – 0.20	0.36 – 0.38	0.54 – 0.57
12:00 – 13:00	0.18	0.35 – 0.36	0.53 – 0.54
13:00 – 14:00	0.18	0.35 – 0.36	0.53 – 0.54
14:00 – 15:00	0.19	0.37 – 0.38	0.56 – 0.58
15:00 – 16:00	0.21 – 0.22	0.42 – 0.43	0.63 – 0.65

Figure 4.15 compares the self consumption values for scenario 3 and the production on 25.03.2014 and 14.06.2014. The production on 25.03.2014 is measured according to UTC+1 and the production on 14.06.2014 is measured according to UTC+2. Consequently, the self consumption factors of the two dates are 1 hour displaced in relation to each other. As seen in

figure 4.15, the self consumption values for example day 25.03.2014 is close to or equal the self consumption values in table 4.9 during morning hours and at noon, but become larger during the afternoon. The self consumption values for each scenario and the production on 25.03.2014 are given in table 4.10.

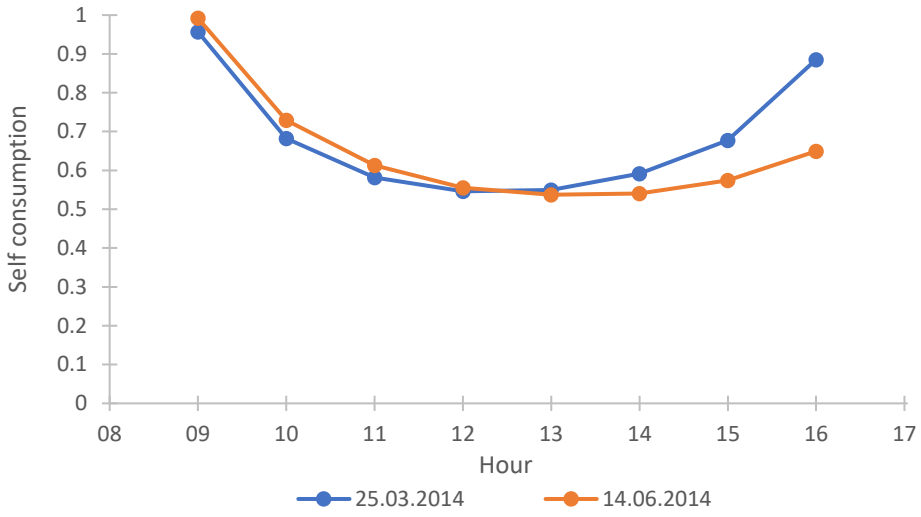

Figure 4.15. The self consumption values of the demand of scenario 3 and the measured production on 25.03.2014 and 14.06.2014.

Table 4.10. Self consumption values for scenario demands and the production on 25.03.2014.

	Scenario 1	**Scenario 2**	**Scenario 3**
08:00 – 09:00	0.32	0.64	0.96
09:00 – 10:00	0.23	0.45	0.68
10:00 – 11:00	0.19	0.39	0.58
11:00 – 12:00	0.18	0.36	0.55
12:00 – 13:00	0.18	0.37	0.55
13:00 – 14:00	0.20	0.39	0.59
14:00 – 15:00	0.22	0.45	0.68
15:00 – 16:00	0.29	0.59	0.89

Table 4.9 and table 4.10 show that the scenario demand cover up to 100 % of the PV production in the morning and up to 55% of the PV production during production peak hours on clear example days.

As already found, the production on clear example day 25.03.2014 and 14.06.2014 is barely sufficient to supply the demand of scenario 3 between 08:00 – 09:00. The simulated clear day profiles are used to investigate how time of year impacts the hourly load match between the clear day production and the demand of scenario 1 and scenario 2. Using the same method as in chapter 4.4.2, it seems that the clear day production between 15.03 – 30.08 is sufficient to supply the hourly demand of scenario 2 and the clear day production between 01.03 – 28.09 is

sufficient to supply the hourly demand of scenario 1. Figure 4.16 illustrates the hourly demand of the scenarios and simulated clear day production in February and March.

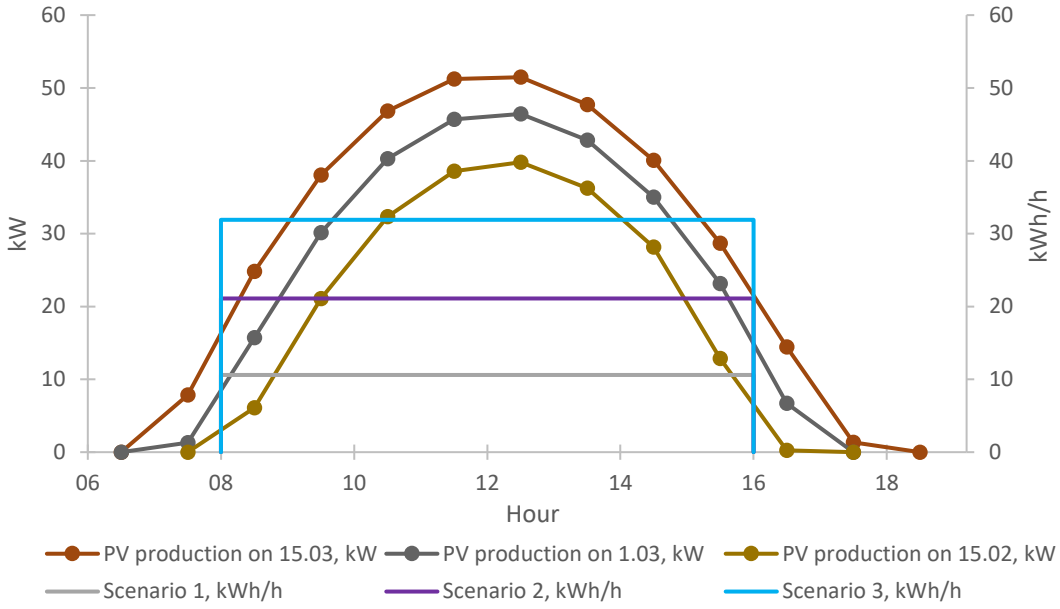

Figure 4.16. Scenario demand and simulated production profiles for February and March.

4.4.5 PV production and scenario demand on cloudy days

Comparing the energy yield of cloudy example days and the energy demand of the scenarios, it is evident that the cloudy example days cannot supply the whole demand of the scenarios. Figure 4.17 illustrates the energy balance between production on 03.02.2016 and the demand of the three scenarios.

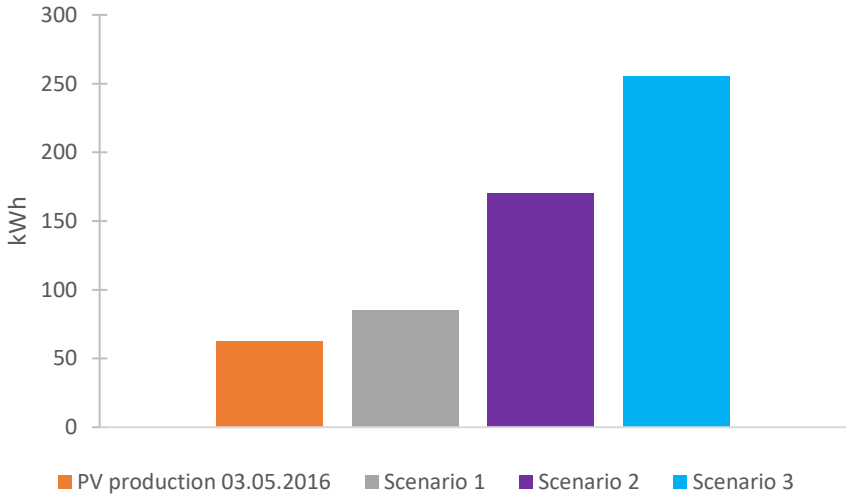

Figure 4.17. Energy balance between production on 03.05.2016 and the demand of the scenarios.

Table 4.11 lists the percentage of days where the daily yield from PV production exceeds the daily energy demand of each scenario from February through November according to PVsyst simulation of a typical year. The daily PV coverage of 21 vehicles charging daily is around 47% in March through September.

Table 4.11. The percentages of days in each month where the daily PV production exceeds the energy demand of the charging scenarios according to PVsyst simulation of a typical year.

	≥ 85 kWh	**≥ 170 kWh**	**≥ 255 kWh**
February, %	43	14	3.6
March, %	81	52	42
April, %	93	90	47
May, %	100	87	55
June, %	93	93	57
July, %	98	84	55
August, %	77	58	39
September, %	83	43	37
October, %	42	29	13
November, %	3	0	0

4.4.6 PV production and fast charging

As already found, every fast charging event lasted for a shorter time than an hour. Consequently, the maximum hourly energy demand is 26 kWh. This demand covers 44 % of the energy production during production peak hour.

Fast charging is characterized by high power demands. The instantaneous power demand may be up to 50 kW which covers up to 85 % of the power peak production seen on clear example days. Instantaneous load match between fast charging DC demand and PV production at Evenstad therefore depends upon a relatively clear sky and that the charging events occurs during production peak hours. Figure 4.18 illustrates the PVsyst simulated spring profiles and the figure marks the hours where the power production is over the found maximum mean power demand of the fast charging events at campus.

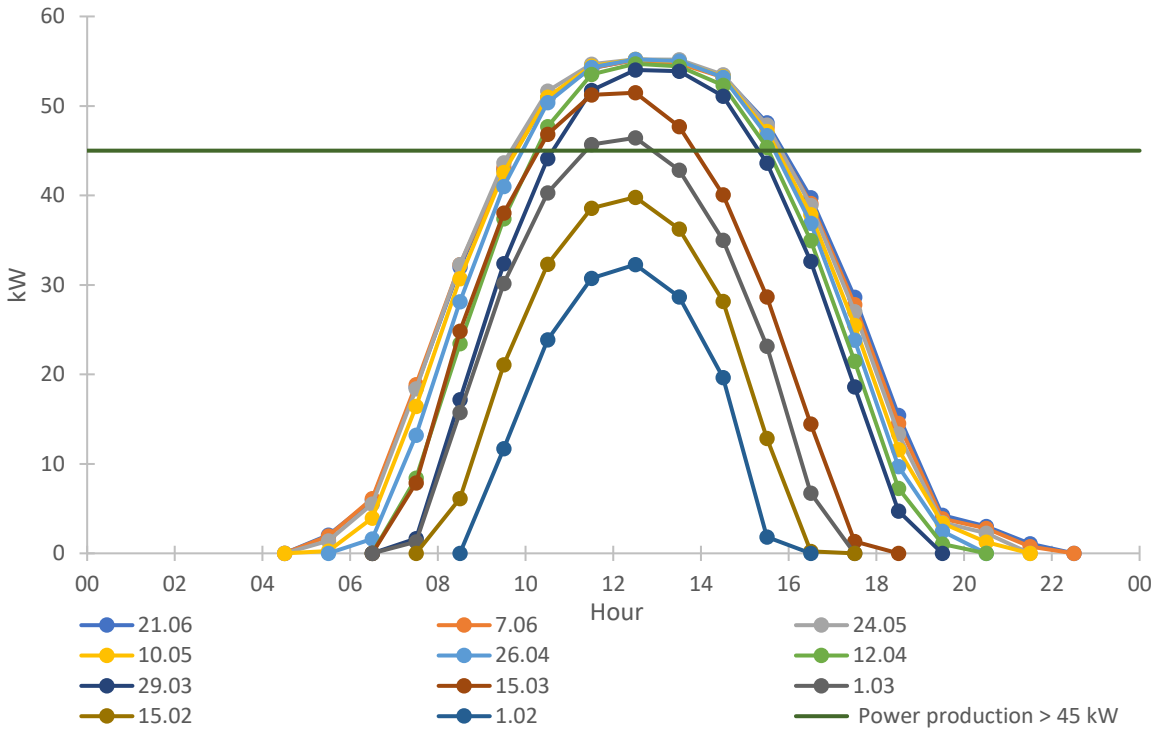

Figure 4.18. The simulated PV production in two-weeks interval from 01.02 – 21.06. The horizontal line marks the hours where the PV production exceeds the maximum mean power demand found in charging data. The maximum mean power demand was 45 kW.

5. Discussion

This chapter discusses different assumptions and findings in previous chapters. In addition, different aspects regarding the measurements and the energy system at Campus Evenstad are discussed.

5.1 PVsyst simulation

5.1.1 Typical year

Since the PV plant has only been operative for four years, it cannot be decided how well the PVsyst simulation represents the monthly production in a typical year. As already mentioned in chapter 3.2.3, Axaopoulos et al [41] have found that PVsyst generally underestimate production due to its implemented PV cell model. While Axaopoulos et al [41] used meteorological data measured on site, the simulation in this thesis uses interpolated meteorological data and interpolated meteorological data adds another uncertainty to the simulation. However, considering that the PVsyst simulated monthly production for February through November is in between or close to the measured monthly production, the simulation seems to correspond well with the monthly production at Campus Evenstad.

5.1.2 Clear days

Although underestimating the production during production peak hours (11.30 -14.30 if UTC+2 and 10.30 – 13.30 if UTC+1), the PVsyst simulation predicts the production profile on clear example days well in the morning before production peak hours and in the afternoon/evening after production peak hours. This is illustrated in figure 4.2 which compares a simulated production profile with a measured production profile.

Simulated production profiles are shifted slightly to the left of the measured production on each clear example days. It may be that the PV array at Campus Evenstad is oriented slightly less towards the East than the surface azimuth angle used for simulations. The daily energy yield does not significantly change if the surface azimuth angle is marginally changed.

5.2 PV production at Campus Evenstad

The PV plant at Campus Evenstad is set up to supply a portion of the energy demand at campus. Campus Evenstad represents both a residential area and a workplace which entails different loads at different times throughout the day. Since the PV array is oriented almost directly towards the South, PV power production coincides first and foremost with work hour load.

Financially, it is more beneficial for the University to locally use the energy produced by the PV plant. Energy producing customers usually pay more when buying energy from the utility than the payment they receive when selling energy to the utility [26]. Whether the PV system supplies the power demand of the buildings or the charging demand at campus does not matter financially since the building load and the charging load are both within the grid connection of the University.

5.3 Charging demand at Campus Evenstad

5.3.1 Slow charging

The selected charging profiles illustrated in figure 4.5 are based on different characteristics of the charging data for April and May 2017. Charging data representing a longer time span than two months is needed to generalize the typical charging demand over a year. EVs use more energy per distance in cold weather and the charging demand probably increase during winter months. Possible seasonable changes in charging demand are not studied due to lack of charging data.

As already stated, the charging demand at campus seems to be work charging. Comparing the three selected charging profiles with the work charging profile presented by NVE in figure 2.10, the peak demand hours correspond. According to figure 2.10, residential charging mainly occurs during the night. No charging events occurred during the night in April and May 2017, but Campus Evenstad represents a special case of residential areas since it is a University campus where most of the residents are students.

Some charging profiles in the dataset are challenging when it comes to make assumptions regarding the number of vehicles charging. If each charging point had been measured separately, the number of vehicles charging had been known. The charging curve for each charging event could have been decided with more certainty if each charging point had been measured in shorter time intervals than an hour.

Nine charging profiles showed a maximum hourly demand of 3.6 – 3.8 kWh/h. Assuming these charging profiles illustrate a single vehicle charging constantly at 3.5 kW, and presupposing the computer generated average power values are representative, the total losses before the power enters the vehicle is 0.1 – 0.3 kWh/h. These losses, which include the Type 2-connector losses, constitute 2.8 – 8.6 %. As mentioned in chapter 2, the Type 2-connector losses are around 5 % [20]. Note that the total charging efficiency is around 89 % according to literature [21].

In some studies [2, 44], an EV-PV charging system entails that the DC power produced by the PV array is directly supplied to the vehicle. At Campus Evenstad, the DC power is converted to AC power before supplying any loads. If supplying the slow charging station, the DC power of the PV array is first converted to AC power by the inverters before being converted back to DC power onboard the vehicle. Such a system includes conversion losses which are avoided if the DC power of the array is supplied directly to the vehicles.

5.3.2 Fast charging

The fast charging data only included measurements of three out of six charging connectors at the fast charging station at campus. It is therefore reasonable to believe that more charging events occurred during the studied time period.

Possible seasonable changes in charging demand is not studied. According to Sintef's measurements from three fast charging stations in Norway over two years, the fast charging demand do not change significantly whether the demand is during the summer, the winter, weekends or weekdays. [25] Like the time distribution of fast charging events presented by NVE in figure 2.10, the fast charging events at Campus Evenstad is distributed throughout the day.

According to the charging curve measurements shown in figure 2.9, the power supply of 50 kW was only delivered for a few minutes before rapidly decreasing. This do not correspond to ABB's measurements since the mean charging power of several charging events were close to 45 kW although lasting for up to 35 minutes. The measurements shown in figure 2.9 are from 2013 and it may be that fast charging curves today are different due to newer charging stations and newer batteries.

The mean charging power and the energy consumption varied by up to 30 kW and 12 kWh respectively on charging events which lasted for approximately the same time. This may be caused by varying charging curves on different charging events according to for example variation of vehicle type and battery condition. Studying the charging events which lasted between 45 – 55 minutes, it seems that the battery was close to SOC 100 % since the mean power and the energy demand were lower compared to many of the charging events which lasted for less than 35 minutes.

The fast charging station at campus is not part of the energy system of the University since Fortum has their own connection to the grid independent of the grid connection of the University. However, accounting for fast charging demand in zero emission neighbourhoods is important.

5.4 Scenario assumptions

Assumptions regarding the amount of energy delivered to each car, the selected energy capacity size of the battery and the time distribution of charging demand are discussed below.

5.4.1 Amount of energy delivered to each vehicle

11.8 kWh was drawn from the grid according to charging profile 1. Assuming the charging efficiency is 89 %, 10.5 kWh was taken up by the battery. The scenarios assume that 10.8 kWh is taken up by the battery since the battery charge 50 % of net energy capacity. The difference between the energy taken up by the battery according to charging profile 1 and the scenarios is 3 %. The choice of energy demand per vehicle in the scenarios is therefore close

to the measured charging demand of charging profile 1 which is assumed to be the charging demand of one vehicle.

5.4.2 Energy capacity size

The scenarios assume that the size of the energy capacity of each vehicle is 21.6 kWh. This size is small compared to the size of other batteries available today and other batteries which will be available in the next few years. Future charging demand in workplaces will depend on future charging patterns, for example how much vehicles are used between each charging event. If the vehicles are used in the same way as seen for charging profile 1, future work charging demand per vehicle may not change despite increasing energy capacity of future EV batteries. Other factors which may play a role in future charging patterns are costs. For example, more people will probably choose to charge their vehicles at work if charging is less expensive at the workplace than at home.

5.4.3 Distribution of charging demand

The scenarios assume that the charging is distributed so that the total charging power is constant throughout eight hours. The resulting power demand is 10.6 kW in scenario 1, 21.2 kW for scenario 2 and 31.9 kW for charging scenario 3. This is an example of controlled charging where the EV load of some vehicles is shifted in time. In contrast, if every vehicle charged simultaneously, the charging demand would last for around 3.3 hours and the total power demand would be 25.8 kW if 7 vehicles charged, 51.6 kW if 14 vehicles charged, and 77.4 kW if 21 vehicles charged. The demand of 21 vehicles charging simultaneously exceeds the rated power of the PV system. The power demand of 14 simultaneously charging vehicles is close to the measured production power peak on clear example days.

Note that the load match between EV charging and PV production can be improved if the charging power is adjusted to the PV production instead of being constant as in the scenarios. This is further discussed in chapter 5.7.

5.5 Annual energy match

The average annual driving length of EVs in 2016 was 16 840 km [45] and the average energy use per kilometre over the year is approximately 0.2 kWh/km [25]. Considering that the specific yield of the PV production at Campus Evenstad is 860 kWh/kWp, a power rating of around 4 kWp is needed to supply the annual energy demand of one vehicle. This constitute around 15 PV modules and around 25 m^2 of the PV array at Campus Evenstad today.

5.6 Time resolution in load match

The load match between demand and production is largely impacted by the time resolution. Different time resolution implies different degrees of self sufficiency although considering the same energy system. In this thesis, hourly load match is emphasized. The University's energy demand and energy export are measured on an hourly basis and the energy invoice is based on these measurements.

Studying load match in shorter time intervals than an hour is interesting to further investigate the reliability of the PV production to cover the EV demand. PV production may have sudden changes due to variation in irradiance caused by clouds. These sudden changes are not represented in energy production measurements given every hour or even 15 minutes. In addition, shorter time intervals than an hour would be helpful to further describe possible increase/decrease in charging power within an hour.

Instantaneous load match is essential in energy systems which are not connected to a backup source such as the grid or a battery.

5.7 Dynamic charging

Dynamic charging refers to variable charging power. Today, dynamic charging management are implemented at different charging stations in Norway. For example, some management systems account for variation in utility prices and some management systems promote load sharing in parking lots to reduce the total power peak demand. [5]

Different studies have investigated how to manage the EV charging power so that the charging power follows the local PV production. These studies have for example looked upon models where the charging power is managed in real-time and/or models where both the PV production and the EV demand are predicted in advance of the charging events. These models aim to increase load match between EV demand and PV production and decrease the need for backup power. [2, 3, 44]

5.8 Smart charging

Utilization of local renewable energy sources is considered a goal for Campus Evenstad as a ZEN pilot and a goal of smart charging according to figure 2.11. Based on charging profile 1, the charging demand of one vehicle lasts for around 4 hours. Assuming that work hours are 8 hours between 07:00 and 17:00, the EV load can be shifted in time in accordance to PV production and still be fully charged by the time the owner needs it to be.

In contrast to slow charging demand, fast charging demand is usually not a flexible load which can be shifted in time. Considering the intermittent nature of PV production, the time

distribution of the fast charging events and the fast charging power peak demand, a connected energy storage is necessary if wanting to cover the fast charging demand by only PV power.

A goal of smart charging is cost-effective management. The University pays the utility according to power tariffs. Consequently, it becomes more cost-effective to charge EVs at a low charging power compared to a higher charging power if the demand is covered by the grid. When managing work charging of for example 7, 14 and 21 vehicles as in the scenarios, it is less expensive to distribute the charging events so that the power drawn from the grid is as low as possible. Considerations regarding utility costs are not necessary if locally produced PV power supplies the whole EV demand.

In a neighbourhood context, the management of EV load also depends on other energy loads in buildings and infrastructure.

6. Conclusions

Campus Evenstad represents both a residential area and a work place. The charging demand at the slow charging station seems to be work charging with charging mainly in the morning. According to three selected charging profiles, the daily energy demand and the maximum hourly demand were up to 45.5 kWh and 12.9 kWh/h respectively.

The rated power of the PV plant is 70 kWp and around 4 kWp is needed to supply the mean annual energy demand of one EV. The PV production at campus coincides with work hour load and the plant produced sufficient energy during charging demand hours to supply the hourly demand of the selected charging profiles on five selected clear days in March through June. According to PVsyst simulation, the PV plant can supply the hourly demand of the selected charging profiles from the middle of March until the middle of September on clear days.

The energy demand of 7, 14 and 21 vehicles which charge daily is 85 kWh, 170 kWh and 255 kWh respectively according to scenario assumptions. The energy demand is distributed over 8 hours between 08:00 – 16:00 and the PV plant can supply the whole hourly demand on every selected clear day in March through June except between 08:00 – 09:00 if 21 vehicles charge daily. In general, the scenario demands covered a larger portion of the hourly PV production than the selected charging profiles. The charging scenarios covered up to 55 % of the peak hour production on selected clear days, while the selected charging profiles covered less than 10 % of the peak hour production on selected clear days.

The load match on cloudy days depends on the cloud cover during demand hours. Adjusting the charging power to the PV production may be necessary to ensure full hourly PV coverage depending on the cloud coverage.

The fast charging demand at campus is distributed throughout the day with most charging events occurring in the afternoon. The maximum energy demand and the maximum mean power demand was 26 kWh and 45 kW respectively. Fast charging is usually not a flexible load which can be shifted in time and a backup power source other than PV power is necessary to ensure full coverage of each charging event.

Work charging load may be shifted in time as long as the vehicles are charged by the end of working hours. Load shifting EV load and adjusting the charging power to the PV production can be used as strategies when optimizing the energy management at Campus Evenstad.

7. Further work

Knowing demand patterns is important in energy management. The slow charging demand at Campus Evenstad presented in this thesis is only based on two months of charging data. The typical charging demand throughout the year can be further investigated by studying charging data covering a longer time span than used in this thesis. In addition, performing measurements of the demand on each charging point in shorter time intervals than an hour decides the charging demand curve of each charging event with more certainty.

Campus Eventad is a pilot area within FME ZEN. Opportunities regarding the energy management at campus will be further investigated by FME ZEN. While this thesis presents a load match analysis of the PV production and the EV load at campus, load match analysis of a wider spectre of energy sources, loads and storages should be studied to decide optimized energy management strategies.

8. References

1. IPCC, *Climate Change 2014: Synthesis Report. Contribution of Working Groups I, II and III to the Fifth Assessment Report of the Intergovernmental Panel on Climate Change.* 2014.
2. Bhatti, A.R., Salam, Z., Aziz, M. J. B., Yee, K. P., Ashique, R. H., *Electric vehicles charging using photovoltaic: Status and technological review.* Renewable & Sustainable Energy Reviews, 2016. **54**: p. 34-47.
3. van der Kam, M., van Sark, W., *Smart charging of electric vehicles with photovoltaic power and vehicle-to-grid technology in a microgrid; a case study.* Applied Energy, 2015. **152**: p. 20-30.
4. OECD/IEA, *Global EV outlook 2017.* 2017.
5. Sørensen, Å.L., *Smart EV charging systems for Zero Emission Neighbourhoods*. 2017 (in press, ZEN project report).
6. Høgskolen i Innlandet. *Om Evenstad*. 2017 [cited 2017, 23.08]; Available from: https://www.inn.no/om-hoegskolen/studiesteder/studiested-evenstad/om-evenstad.
7. Sørensen, Å.L., Fredriksen, E., Walnum, H. T., Andresen, I., Skeie, K. S., *ZEN pilot survey WP4 Energy flexible neighbourhoods.* 2017, Memo in FME ZEN (in press).
8. Smets, A., Jäger, K., Isabella, O., van Swaaij, R., Zeman, M., *Solar Energy - The physics and engineering of photovoltaic conversion technologies and systems*. 2016: UIT Cambridge Ltd.
9. Honsberg, C., Bowden, S. *PVeducation.org*. 2014 [cited 2017, 25.08]; Available from: http://www.pveducation.org/.
10. Seaward. *Curve tracing FAQ's*. [cited 2017, 30.10]; Available from: http://www.seaward-groupusa.com/userfiles/curve-tracing.php.
11. Burger, B., Kiefer, K., Kost, C., Nold, S., Philipps, S., Preu, R., Rentsch, J., Schlegl, T., Stryi-Hipp, G., Willeke, G et. al., *Photovoltaics Report*. 2016, Fraunhofer ISE.
12. Åsheim, T.B., *Analysis of a Photovoltaic Power Plant at Evenstad*. MSc. 2017, Norwegian University of Science and Technology.
13. SMA Solar Technology AG. *PV Inverters - Basic Facts for Planning PV Systems*. [cited 2017, 30.10]; Available from: https://www.sma.de/en/partners/knowledgebase/%20pv-inverters-basic-facts-for-planning-pv-systems.html.
14. Understandsolar. *Solar Inverter Efficiency – What is the Most Efficient Solar Inverter?* [cited 2017, 27.11]; Available from: https://understandsolar.com/solar-inverter-efficiency/.
15. Kjaer, S.B., Pedersen, J. K., Blaabjerg, F., *A review of single-phase grid-connected inverters for photovoltaic modules.* IEEE Transactions on Industry Applications, 2005. **41**(September/October 2005).
16. Chen, J.C., *Physics of solar energy* 2011, New Jersey: John Wiley & Sons.
17. Øgaard, M.B., *Effect of Soiling on the Performance of Photovoltaic Modules in Kalkbult, South Africa*. MSc. 2016, Norwegian University of Life Sciences.
18. Massachusetts Institute of Technology. *A Guide to Understanding Battery Specifications*. 2008 [cited 2017 13.09]; Available from: http://web.mit.edu/evt/summary_battery_specifications.pdf.
19. Fjordkraft. *Hva er hurtiglading?* [cited 2017, 4.12]; Available from: https://www.ladestasjoner.no/hurtiglading/hva-er-hurtiglading/.
20. Moberg, K. *Elbil-fremtid uten stikkontakt?* 2017 [cited 2017, 13.11]; Available from: http://www.dinside.no/motor/elbil-fremtid-uten-stikkontakt/67618116.

21. Sears, J., Roberts, D., Glitman, K., *A comparison of electric vehicle Level 1 and Level 2 charging efficiency*. Technologies for Sustainability (SusTech) 2014 IEEE Conference, 2014.
22. Aunedi, M., Woolf, M., Bilton, Strbac, G., *Impact and opportunities for wide-scale electric vehicle deployment*. 2014, Report B1 for the "Low Carbon London" LNCF project: Imperial College London.
23. Brendryen, A., (Fortum), *email dialog*. 2017.
24. Seljeseth, H., Taxt, H., *Elbilers ladeforløp og utfordringer for el-nettet*. 2013, Report number TR A7332, Sintef.
25. Skotland, H.C., Eggum, E., Spilde, D., *Hva betyr elbiler for strømnettet?* 2016, report number 74-2016, NVE.
26. Sørensen, Å.L., Sartori, I., Andresen, I., *Smart EV Charging Systems to Improve Energy Flexibility of Zero Emission Neighbourhoods: A state-of-the-art for Norway*. 2017 (in press for conference Cold Climate HVAC 2018).
27. Valle, M. *Dette er elbilene som kommer de neste to årene*. 2017 [cited 2017, 03.11]; Available from: https://www.tu.no/artikler/dette-er-elbilene-som-kommer-de-neste-to-arene/409284.
28. Salom, J., Marszal, A. J., Candanedo, J., Widén, J., Lindberg, K. B., Sartori, I. , *Analysis Of Load Match and Grid Interaction Indicators in NZEB with High-Resolution Data*. 2014, IEA-SHC Task 40/Annex 52, Towards Net Zero Energy Solar Buildings.
29. Statsbygg. *Seminar om solceller 18.11.2013*. 2013 [cited 2017, 25.08]; Available from: http://slideplayer.no/slide/2028103/.
30. Sørensen, Å.L., *Dialog*. 2017.
31. REC. *Data sheet*. [cited 2017, 25.08]; Available from: http://www.recgroup.com/sites/default/files/documents/datasheet_rec_peak_energy_blk_us_rev_v_eng.pdf.
32. Fornybar.no. *5. Eksempelprosjekter*. [cited 2017, 26.09]; Available from: http://www.fornybar.no/solenergi/eksempelprosjekter.
33. Sønnico, *FDV dokumentasjon* Prosjekt: Solenergianlegg Evenstad, 2014.
34. SMA Solar Technology AG. *Data sheet*. [cited 2017, 01.09]; Available from: http://files.sma.de/dl/15330/SB5000TL-21-DEN1551-V20web.pdf.
35. FUSen, *Elektro oversikt Evenstad*. 2014.
36. Salto, *LADE informasjon*. Sign at the slow charging station at Campus Evenstad.
37. Eng-Øvermo, T., (Statsbygg), *Dialog*. 2017.
38. ABB and Efacec Electric Mobility, *Techincal specifications*. Signs at the fast charging station at Campus Evenstad.
39. PVsyst. *Meteonorm data and program*. [cited 2017, 24.11]; Available from: http://files.pvsyst.com/help/meteo_source_meteonorm.htm.
40. REC Solar ASA. *Assessing reflection from rec peak energy series panels*. 2014 [cited 2017, 1.10]; Available from: http://www.recgroup.com/sites/default/files/documents/reflectivity_and_iam.pdf.
41. Axaopoulos, P., Fylladitakis, E., Gkarakis, K., *Accuracy analysis of software for the estimation and planning of photovoltaic installations.* International Journal of Energy and Environmental Engineering, 2014. **5**(1): p. 1-7.
42. SMA Solar Technology AG. *Measurement accuracy, Energy values and efficiency for PV Inverter Sunny Boy and Sunny Mini Central*. [cited 2017, 14.11]; Available from: http://files.sma.de/dl/7418/Messgenau-UEN092520.pdf.
43. Piene, E.F., (Salto), *email dialog*. 2017.

44. Mouli, G.R.C., Bauer, P., Zeman, M., *System design for a solar powered electric vehicle charging station for workplaces.* Applied Energy, 2016. **168**: p. 434-443.
45. Statistisk sentralbyrå. *Vi kjører mer i stadig flere biler*. 2017 [cited 2017, 3.12]; Available from: https://www.ssb.no/transport-og-reiseliv/artikler-og-publikasjoner/vi-kjorer-mer-i-stadig-flere-biler.

9. Appendix

Appendix A: PVsyst simulation report of a typical year

Appendix B: PVsyst simulated power production on clear days

Appendix C: Charging demand at the slow charging station

Appendix A

Grid-Connected System: Simulation parameters

Project :	**Campus Evenstad**			
Geographical Site	**Evenstad**		Country	**Norway**
Situation	Latitude	61.42° N	Longitude	11.08° E
Time defined as	Legal Time	Time zone UT+1	Altitude	260 m
	Albedo	0.20		
Meteo data:	**Evenstad**	Meteonorm 7.1 (1991-2010), Sat=79% - Synthetic		

Simulation variant : **normal, detailed losses, a = 10**

Simulation date 20/10/17 10h07

Simulation parameters

Collector Plane Orientation	Tilt	35°	Azimuth	-10°
Models used	Transposition	Hay	Diffuse	Perez, Meteonorm
Horizon	Average Height	5.0°		
Near Shadings	Detailed electrical calculations	(acc. to module layout)		

PV Arrays Characteristics (2 kinds of array defined)

PV module	Si-poly Model	**REC 255PE / PE-BLK**		
Original PVsyst database	Manufacturer	REC		
Sub-array "Sub-array #1"				
Number of PV modules	In series	11 modules	In parallel	12 strings
Total number of PV modules	Nb. modules	132	Unit Nom. Power	255 Wp
Array global power	Nominal (STC)	**33.7 kWp**	At operating cond.	30.3 kWp (50°C)
Array operating characteristics (50°C)	U mpp	302 V	I mpp	100 A
Sub-array "Sub-array #1"				
Number of PV modules	In series	12 modules	In parallel	12 strings
Total number of PV modules	Nb. modules	144	Unit Nom. Power	255 Wp
Array global power	Nominal (STC)	**36.7 kWp**	At operating cond.	33.0 kWp (50°C)
Array operating characteristics (50°C)	U mpp	329 V	I mpp	100 A
Total Arrays global power	Nominal (STC)	**70 kWp**	Total	276 modules
	Module area	**455 m²**	Cell area	403 m²

Inverter	Model	**Sunny Boy 5000 TL-21**		
Original PVsyst database	Manufacturer	SMA		
Characteristics	Operating Voltage	175-500 V	Unit Nom. Power	4.60 kWac
Sub-array "Sub-array #1"	Nb. of inverters	12 * MPPT 50 %	Total Power	28 kWac
Sub-array "Sub-array #1"	Nb. of inverters	12 * MPPT 50 %	Total Power	28 kWac
Total	Nb. of inverters	12	Total Power	55 kWac

PV Array loss factors

Thermal Loss factor	Uc (const)	20.0 W/m²K	Uv (wind)	0.0 W/m²K / m/s
Wiring Ohmic Loss	Array#1	50 mOhm	Loss Fraction	1.5 % at STC
	Array#2	54 mOhm	Loss Fraction	1.5 % at STC
	Global		Loss Fraction	1.5 % at STC
LID - Light Induced Degradation			Loss Fraction	1.5 %
Module Quality Loss			Loss Fraction	-0.5 %
Module Mismatch Losses			Loss Fraction	1.0 % at MPP

Grid-Connected System: Simulation parameters (continued)

Incidence effect, user defined profile

0°	30°	50°	60°	70°	75°	80°	85°	90°
1.00	1.00	0.99	0.97	0.91	0.84	0.72	0.48	0.00

User's needs : Unlimited load (grid)

Grid-Connected System: Horizon definition

Project : **Campus Evenstad**

Simulation variant : **normal, detailed losses, a = 10**

Main system parameters		System type	**Grid-Connected**		
Horizon		Average Height	5.0°		
Near Shadings		Detailed electrical calculations	(acc. to module layout)		
PV Field Orientation		tilt	35°	azimuth	-10°
PV modules		Model	REC 255PE / PE-BLK	Pnom	255 Wp
PV Array		Nb. of modules	276	Pnom total	**70.4 kWp**
Inverter		Model	Sunny Boy 5000 TL-21	Pnom	4600 W ac
Inverter pack		Nb. of units	12.0	Pnom total	**55.2 kW ac**
User's needs		Unlimited load (grid)			

Horizon

Average Height	5.0°	Diffuse Factor	0.97
Albedo Factor	100 %	Albedo Fraction	0.84

Height [°]	11.0	11.0	13.0	12.0	11.0	9.0	7.0	6.0	5.0	5.0	4.0	1.0	0.0	0.2
Azimuth [°]	-180	-179	-178	-166	-158	-148	-144	-135	-123	-90	-80	-61	-49	-45
Height [°]	2.0	4.0	5.0	6.0	7.0	7.0	3.0	3.0	4.0	4.0	6.0	11.0	11.0	
Azimuth [°]	-11	0	10	31	45	54	90	116	135	138	162	179	180	

Meteonorm horizon for, Lat. = 61.424°, Long.Legal Time

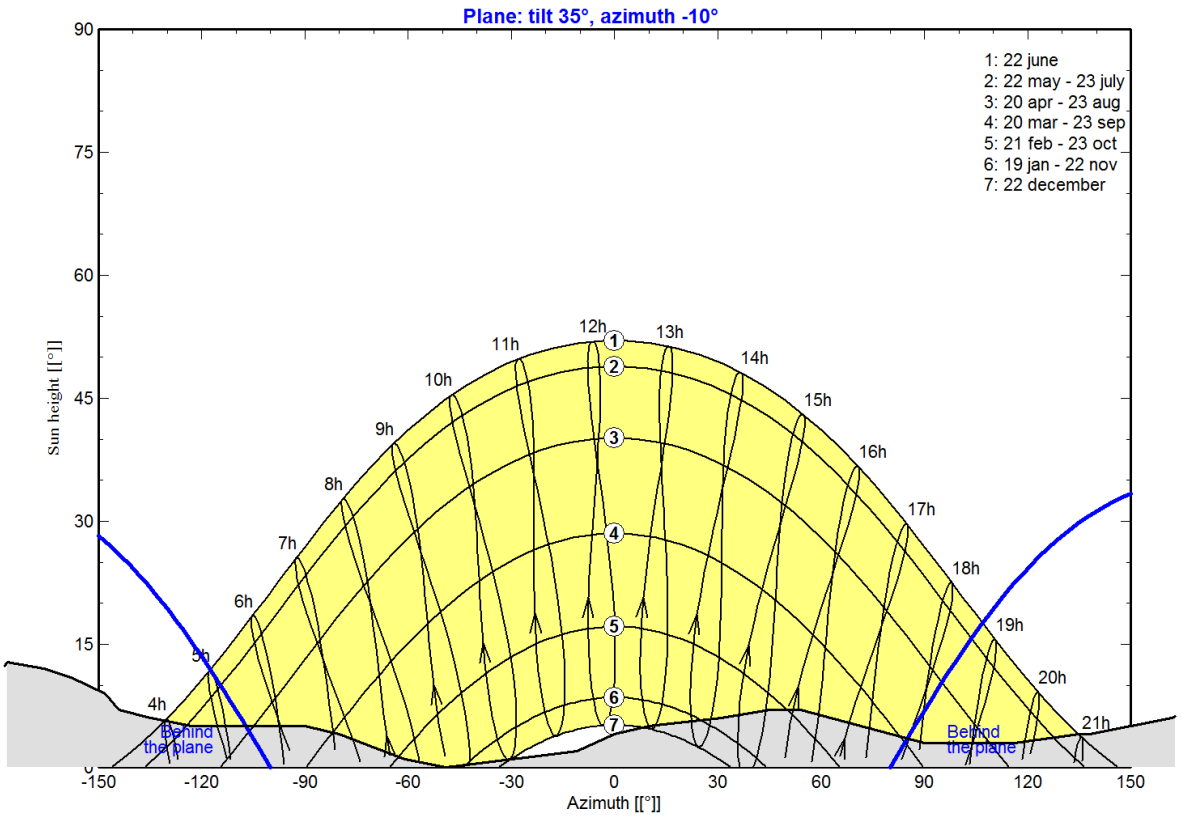

Grid-Connected System: Near shading definition

Project : **Campus Evenstad**

Simulation variant : **normal, detailed losses, a = 10**

Main system parameters		System type	**Grid-Connected**		
Horizon		Average Height	5.0°		
Near Shadings		Detailed electrical calculations	(acc. to module layout)		
PV Field Orientation		tilt	35°	azimuth	-10°
PV modules		Model	REC 255PE / PE-BLK	Pnom	255 Wp
PV Array		Nb. of modules	276	Pnom total	**70.4 kWp**
Inverter		Model	Sunny Boy 5000 TL-21	Pnom	4600 W ac
Inverter pack		Nb. of units	12.0	Pnom total	**55.2 kW ac**
User's needs		Unlimited load (grid)			

Perspective of the PV-field and surrounding shading scene

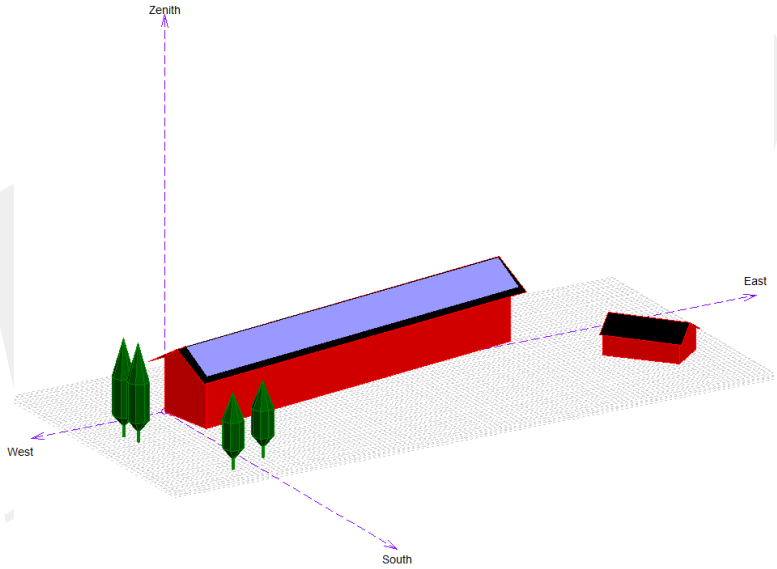

Iso-shadings diagram

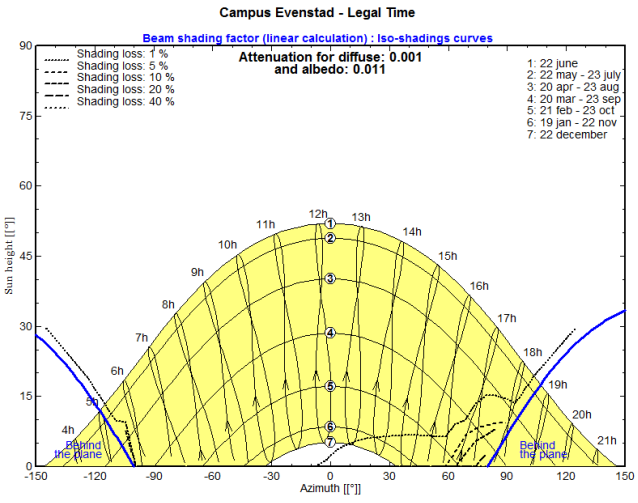

Grid-Connected System: Main results

Project : **Campus Evenstad**

Simulation variant : **normal, detailed losses, a = 10**

Main system parameters	System type	**Grid-Connected**			
Horizon	Average Height	5.0°			
Near Shadings	Detailed electrical calculations	(acc. to module layout)			
PV Field Orientation	tilt	35°	azimuth	-10°	
PV modules	Model	REC 255PE / PE-BLK	Pnom	255 Wp	
PV Array	Nb. of modules	276	Pnom total	**70.4 kWp**	
Inverter	Model	Sunny Boy 5000 TL-21	Pnom	4600 W ac	
Inverter pack	Nb. of units	12.0	Pnom total	**55.2 kW ac**	
User's needs	Unlimited load (grid)				

Main simulation results

System Production

Produced Energy	**61629 kWh/year**	Specific prod.	876 kWh/kWp/year
Performance Ratio PR	85.91 %		

Normalized productions (per installed kWp): Nominal power 70.4 kWp

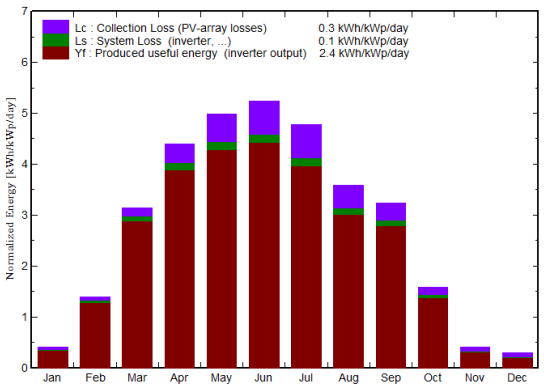

Performance Ratio PR

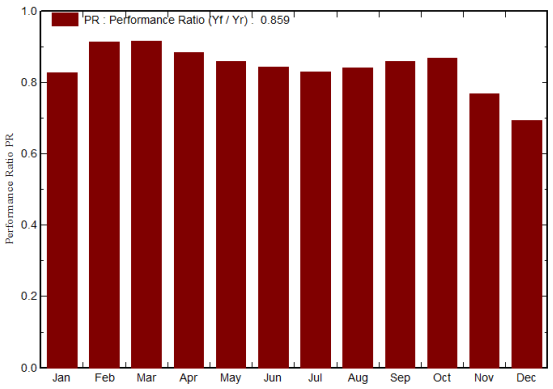

normal, detailed losses, a = 10

Balances and main results

	GlobHor kWh/m²	T Amb °C	GlobInc kWh/m²	GlobEff kWh/m²	EArray kWh	E_Grid kWh	EffArrR %	EffSysR %
January	5.8	-5.90	12.7	11.4	790	741	13.65	12.81
February	20.3	-5.80	39.1	37.2	2626	2515	14.75	14.13
March	61.2	-2.10	97.4	94.4	6519	6287	14.69	14.17
April	105.3	4.10	131.9	127.3	8503	8203	14.16	13.66
May	144.1	9.30	154.4	148.6	9693	9342	13.79	13.29
June	154.1	13.30	157.3	151.3	9697	9336	13.53	13.03
July	142.8	16.10	148.1	142.3	8988	8648	13.33	12.82
August	98.8	14.70	111.2	107.0	6852	6584	13.53	13.00
September	68.4	9.80	97.1	94.0	6114	5883	13.82	13.30
October	27.7	3.70	49.0	46.9	3133	2994	14.04	13.42
November	7.1	-1.00	12.0	10.4	707	649	12.94	11.89
December	3.2	-6.00	9.1	6.9	474	444	11.46	10.74
Year	838.8	4.24	1019.3	977.6	64094	61629	13.81	13.28

Legends:

GlobHor	Horizontal global irradiation	EArray	Effective energy at the output of the array
T Amb	Ambient Temperature	E_Grid	Energy injected into grid
GlobInc	Global incident in coll. plane	EffArrR	Effic. Eout array / rough area
GlobEff	Effective Global, corr. for IAM and shadings	EffSysR	Effic. Eout system / rough area

Grid-Connected System: Loss diagram

Project : **Campus Evenstad**

Simulation variant : **normal, detailed losses, a = 10**

Main system parameters	System type	**Grid-Connected**			
Horizon	Average Height	5.0°			
Near Shadings	Detailed electrical calculations	(acc. to module layout)			
PV Field Orientation	tilt	35°	azimuth	-10°	
PV modules	Model	REC 255PE / PE-BLK	Pnom	255 Wp	
PV Array	Nb. of modules	276	Pnom total	**70.4 kWp**	
Inverter	Model	Sunny Boy 5000 TL-21	Pnom	4600 W ac	
Inverter pack	Nb. of units	12.0	Pnom total	**55.2 kW ac**	
User's needs	Unlimited load (grid)				

Loss diagram over the whole year

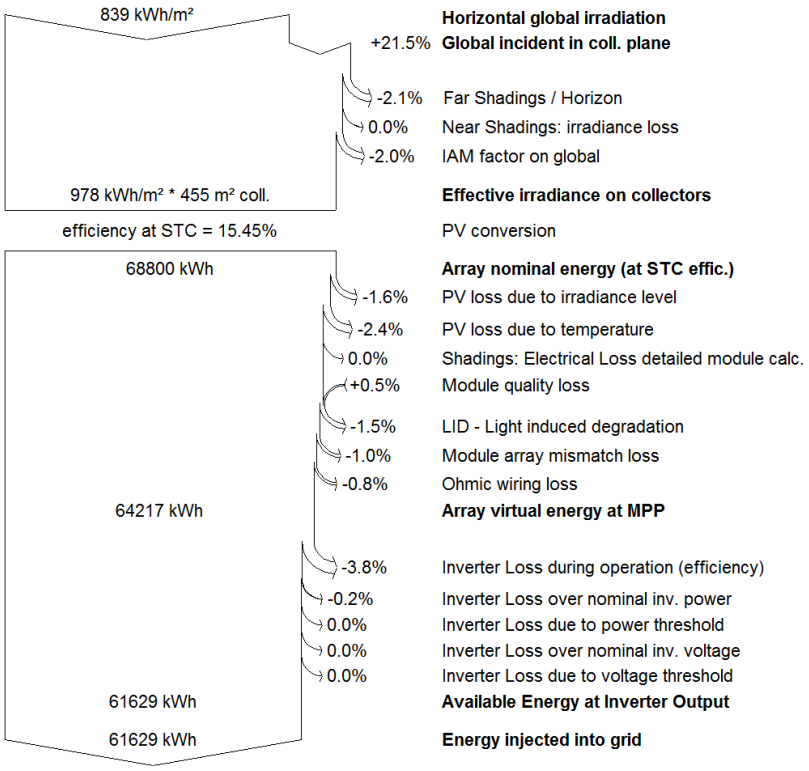

Appendix B

The power production on PVsyst simulated clear days in two-weeks interval is given in table 0.1 – 0.2. Each value is given in kW.

Table 0.1. The instantaneous power values of PVsyst simulated clear days from 1.2 – 21.6 where each value is given in kW.

Time	**1.2**	**15.2**	**1.3**	**15.3**	**29.3**	**12.4**	**26.4**	**10.5**	**24.5**	**7.6**	**21.6**
05.30								0.26	1.4	1.9	2.0
06:30							1.6	3.9	5.5	6.1	6.0
07:30			1.3	7.9	1.7	8.4	13	16	18	19	19
08:30		6.1	16	25	17	23	28	31	32	32	32
09:30	12	21	30	38	32	37	41	43	44	43	43
10:30	24	32	40	47	44	48	50	51	52	51	51
11:30	31	39	46	51	52	54	54	54	55	54	54
12:30	32	40	46	51	54	55	55	55	55	55	55
13:30	29	36	43	48	54	54	55	55	55	55	55
14:30	20	28	35	40	51	52	53	53	53	53	53
15:30	1.8	13	23	29	43	45	47	47	48	48	48
16:30		0.23	6.7	14	33	35	37	38	39	39	40
17:30				1.8	19	21	24	25	27	28	29
18:30					4.7	7.3	9.7	12	13	15	15
19:30						1.1	2.5	3.4	3.4	3.9	4.3
20:30								1.2	2.3	2.8	3.0
21:30										0.76	1.1

Table 0.2. The instantaneous power values of PVsyst simulated clear days from 5.7 – 8.11 where each value is given in kW.

Time	**5.7**	**19.7**	**2.8**	**16.8**	**30.8**	**13.9**	**28.9**	**11.10**	**25.10**	**8.11**
05.30	1.7	1.0								
06:30	5.2	4.1	2.7	1.1						
07:30	17	16	14	11	8.3	3.7	0.43			
08:30	31	29	28	26	23	19	14	5.6		5.8
09:30	42	41	40	38	36	33	28	22	14	19
10:30	50	49	48	47	45	43	39	34	27	28
11:30	54	54	53	53	51	50	46	42	35	32
12:30	55	55	54	54	53	53	49	45	39	31
13:30	54	54	54	54	53	52	48	44	38	25
14:30	53	53	53	52	50	48	44	39	32	9.4
15:30	48	47	47	46	43	40	35	30	22	
16:30	39	39	38	37	33	30	24	17	4.8	
17:30	29	28	27	24	21	16	10	2.0		
18:30	16	15	13	11	7.2	3.4	0.07			
19:30	4.3	3.0	3.3	2.7	1.1					
20:30	2.9	2.5	1.7	0.25						
21:30	0.97	0.39								

Appendix C

The computer generated average power values of the charging demand at the slow charging station is shown in table 0.3 – 0.5. Altogether, the tables show the 26 charging profiles in April and May 2017 that were the basis for selecting the charging profiles which were used in load match analysis.

Each value describes the demand of the previous hour and each value are given in kWh/h.

Table 0.3. The computer generated average power values of charging profiles between 1.4.2017 – 26.4.2017. Each value is given in kWh/h and each value describes the demand of the previous hour.

Hour	3.4.17	4.4.17	5.4.17	6.4.17	7.4.17	18.4.17	19.4.17	20.4.17	26.4.17
06									
07								3.5	
08		2.0	2.2		3.6	4.6	3.5	8.4	1.9
09		3.7	3.7		3.6	10.1	8.3	11.9	3.5
10		3.7	3.7	1.9		10.1	6.8	10.4	3.5
11	2.0	2.3	3.7	3.6		5.4	3.5	6.0	3.5
12	3.7		2.6	6.8	2.0	1.5	2.9	4.3	3.5
13	3.8		0.9	3.6	3.7	1.0	1.8	3.7	3.5
14	3.8			1.9	2.6			3.7	3.5
15	3.8			0.5	0.9			3.1	2.5
16	3.8							1.9	0.9
17	3.2								
18	1.5								

Table 0.4. The computer generated average power values of charging profiles between 27.4.2017 – 12.5.2017. Each value is given in kWh/h. Each value is given in kWh/h and each value describes the demand of the previous hour.

Hour	27.4.17	28.4.17	2.5.17	3.5.17	5.5.17	8.5.17	9.5.17	11.5.17	12.5.17
06									
07							3.5		
08	1.9	1.9	4.0	2.2	3.8		8.5	3.8	1.9
09	3.5	8.3	7.3	3.5	7.3	3.5	10.4	7.3	3.6
10	3.5	6.8	6.1	3.5	6.3	6.8	7.2	10.1	3.6
11	2.5	3.5	3.8	2.5	1.9	3.5	6.0	8.4	2.0
12	0.9	2.9	1.3	0.9			5.5	5.2	0.7
13		1.8					3.7	4.3	
14							3.7	2.3	
15							3.2	1.3	
16							1.4		
17									
18									

Table 0.5. The computer generated average power values of charging profiles between 13.5.2017 – 31.5.2017. Each value is given in kWh/h and each value describes the demand of the previous hour.

Hour	**15.5.17**	**16.5.17**	**18.5.17**	**19.5.17**	**22.5.17**	**23.5.17**	**30.5.17**	**31.5.17**
06								
07	2.1					1.9		
08	5.6	1.9	3.6	2.3	3.7	5.4	5.4	2.0
09	6.8	9.2	10.6	3.5	7.1	10.5	10.6	3.6
10	5.2	13.8	12.9	3.5	7.1	11.6	10.1	3.6
11	4.0	8.0	8.2	2.5	4.8	7.0	8.2	3.6
12	1.9	4.4	4.2	0.8	1.3	3.2	6.2	6.9
13		3.6	3.6				4.6	10.2
14		2.4	2.4				2.2	3.6
15		0.8					0.7	
16								
17								
18								

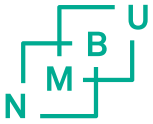

Norges miljø- og biovitenskapelige universitet
Noregs miljø- og biovitskapelege universitet
Norwegian University of Life Sciences

Postboks 5003
NO-1432 Ås
Norway